

MOST[®]

Media Oriented Systems Transport

Multimedia and Control
Networking Technology

Application Note POF Transfer Function

Rev. 1.1

11/2010

MOSTCO CONFIDENTIAL

See page 3 for the terms of disclosure



Legal Notice

COPYRIGHT

© Copyright 1999 - 2010 MOST Cooperation. All rights reserved. Duplication of this document without permission is prohibited. The information within this document is confidential and MOST Cooperation intellectual property.

LICENSE DISCLAIMER

Nothing on any MOST Cooperation Web Site, or in any MOST Cooperation document, shall be construed as conferring any license under any of the MOST Cooperation or its members or any third party's intellectual property rights, whether by estoppel, implication, or otherwise.

CONTENT AND LIABILITY DISCLAIMER

MOST Cooperation or its members shall not be responsible for any errors or omissions contained at any MOST Cooperation Web Site, or in any MOST Cooperation document, and reserves the right to make changes without notice. Accordingly, all MOST Cooperation and third party information is provided "AS IS". In addition, MOST Cooperation or its members are not responsible for the content of any other Web Site linked to any MOST Cooperation Web Site. Links are provided as Internet navigation tools only.

MOST COOPERATION AND ITS MEMBERS DISCLAIM ALL WARRANTIES WITH REGARD TO THE INFORMATION (INCLUDING ANY SOFTWARE) PROVIDED, INCLUDING THE IMPLIED WARRANTIES OF MERCHANTABILITY AND FITNESS FOR A PARTICULAR PURPOSE, AND NON-INFRINGEMENT. Some jurisdictions do not allow the exclusion of implied warranties, so the above exclusion may not apply to you.

In no event shall MOST Cooperation or its members be liable for any damages whatsoever, and in particular MOST Cooperation or its members shall not be liable for special, indirect, consequential, or incidental damages, or damages for lost profits, loss of revenue, or loss of use, arising out of or related to any MOST Cooperation Web Site, any MOST Cooperation document, or the information contained in it, whether such damages arise in contract, negligence, tort, under statute, in equity, at law or otherwise.

FEEDBACK INFORMATION

Any information provided to MOST Cooperation in connection with any MOST Cooperation Web Site, or any MOST Cooperation document, shall be provided by the submitter and received by MOST Cooperation on a non-confidential basis. MOST Cooperation shall be free to use such information on an unrestricted basis.

TRADEMARKS

MOST Cooperation and its members prohibit the unauthorized use of any of their trademarks. MOST Cooperation specifically prohibits the use of the MOST Cooperation LOGO unless the use is approved by the Steering Committee of MOST Cooperation.

SUPPORT AND FURTHER INFORMATION

For more information on the MOST technology, please contact:

MOST Cooperation
Administration
Bannwaldallee 48
D-76185 Karlsruhe
Germany
Phone: (+49) (0) 721 966 50 00
E-mail: contact@mostcooperation.com
Web: www.mostcooperation.com



This Specification is Confidential Information of the MOST Cooperation. It may only be disclosed to member companies. Member companies wishing to discuss these Specifications with suppliers or other third parties must ensure that a commercially standard form of non-disclosure agreement has been previously executed by the party receiving such Specifications. Use of these Specifications may only be for purposes for which they are intended by the MOST Cooperation. Unauthorized use or disclosure is a violation of law.

© Copyright 1999 - 2010 MOST Cooperation
All rights reserved

MOST is a registered trademark

Contents

1	BIBLIOGRAPHY	5
2	DOCUMENT HISTORY.....	5
3	INTRODUCTION.....	6
4	FUNDAMENTAL TRANSFER FUNCTION OF THE POF.....	7
4.1	Low Pass Characteristic	7
4.2	Mathematical Description	7
5	TRANSFER FUNCTION DEPENDENT ON POF-LENGTH.....	9
6	TRANSFER FUNCTION DEPENDENT ON LAUNCHING APERTURE.....	17
7	USING MODEL EQUATIONS	20
8	CONCLUSION	21
9	REFERENCES.....	21
10	APPENDIX: EVALUATION RESULTS FOR 15M POF AND LAUNCHING APERTURE 0.5 ...	22
10.1	SIM slow.....	22
10.2	SIM ov	25
10.3	SIM tst	28
10.4	A set of rules for calculation	30
10.5	MATLAB script for calculation of SP3-signal	32
11	APPENDIX: AUTOMATED DETERMINATION OF WORST-CASE SCENARIOS FOR THE MOST OPTICAL PHYSICAL LAYER SPECIFICATION POINT 3.....	34
11.1	Introduction	34
11.2	SP3 Input Pattern Calculation.....	34
11.2.1	Rising and Falling Edge Generation.....	34
11.2.2	Combining the Rising and Falling Edge with a pre-defined Bit-Pattern	36
11.3	Calculation of the SP3 Pattern	37
11.4	Simulation and Analysis	38
11.5	Results	39
12	APPENDIX A: INDEX OF FIGURES	43
13	APPENDIX B: INDEX OF TABLES	44

1 Bibliography

Number	Document
[1]	MOST Specification Rev 3.0
[2]	MOST Physical Layer Basic Specification Rev. 1.0
[3]	MOST150 oPHY Automotive Physical Layer Sub-Specification Rev. 1.1

Table 1-1 Bibliography

2 Document History

Changes from Rev. 1.0 to Rev. 1.1

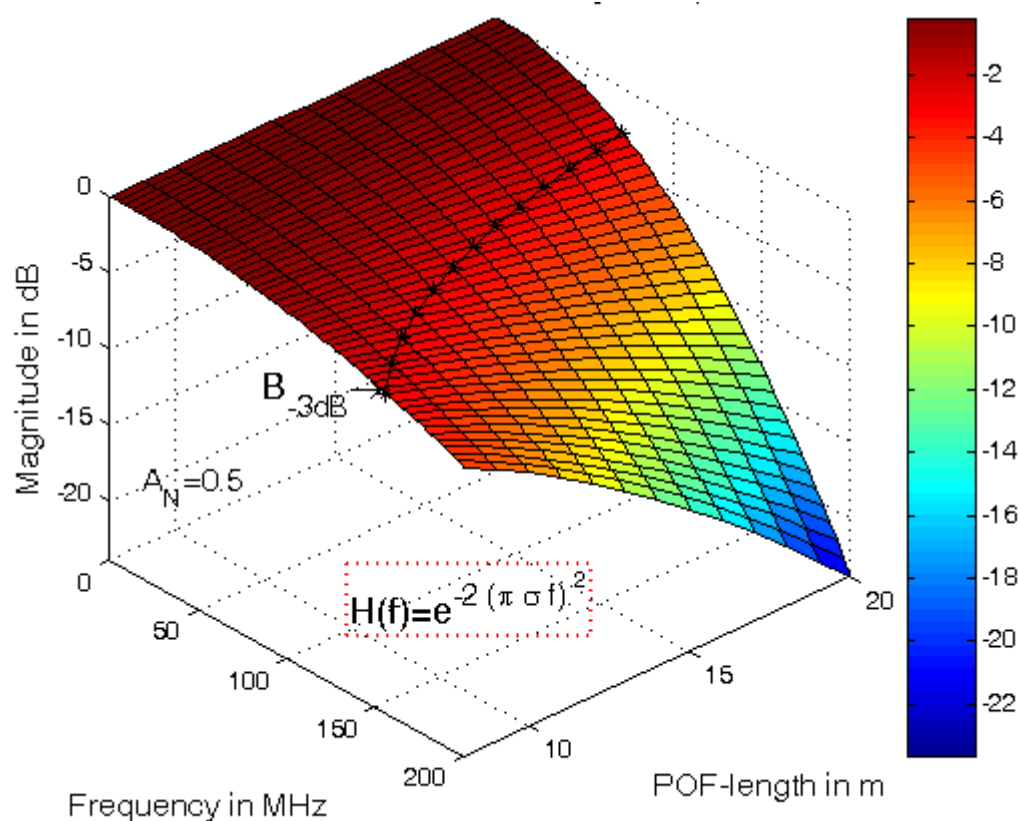
Revision	Changes
1.1	Chapter 11 added

Rev. 1.0

Revision	Changes
1.0	First issue (Dec. 2008)

3 Introduction

This report investigates the baseband frequency and time responses of a polymer optic fiber (POF) as a linear time invariant system. Thus, the system baseband impulse response and transfer function can be calculated in terms of the individual component baseband impulse and frequency responses. This is accomplished by generating a general relationship of the polymer fiber's transfer function dependent on the fiber length and the launching condition at the fiber input. This transfer function should be simple but sufficiently accurate to predict the system performance. The transfer function enables realistic analyses to be performed in order to define the limits of performance of the system more clearly.



4 Fundamental Transfer Function of the POF

4.1 Low Pass Characteristic

The capability to transmit high frequency signals can be observed by the deformation of short pulses travelling down the fiber or by the fiber bandwidth if the frequency response characteristic is defined. Both are influenced by numerous effects, e.g., light source properties and launching conditions, fiber dispersion (in this case only modal dispersion), mode mixing in the fiber, nonuniform mode attenuation, and by statistical variations of all these effects along the fiber.

We assume that the light source emits very short pulse, i.e., the frequency spectrum of this pulse is much broader than the supposed POF bandwidth. Because of the modal dispersion the launched pulse splits up in a high number of modes each arriving at the fiber end statistical distributed around a fiber length dependent average group delay. The photodiode superposes the responses of all modes. If we interpret the output pulse of each mode as a probability density function of a random variable instead of its temporal shape the application of the Central Limit Theorem leads to the consequence that the pulse response of the POF must be well approximated by a Gaussian shape. Thus, the transfer function must be Gaussian too.

4.2 Mathematical Description

It is well known that a light pulse can be described by its temporal shape $h(t)$ and $h(t)$ is characterized by the temporal moments of the pulse as the area (zero order moment)

$$A = \int_{-\infty}^{+\infty} h(t) dt \quad (4.1)$$

the central time (first order moment or group delay)

$$t_c = \frac{1}{A} \int_{-\infty}^{+\infty} t \cdot h(t) dt \quad (4.2)$$

and the m^{th} order central moments

$$M_m = \frac{1}{A} \int_{-\infty}^{+\infty} (t - t_c)^m \cdot h(t) dt \quad (4.3)$$

Certainly, the most important central moment is $M_2 = \sigma^2$, which equals the variance and characterizes the temporal width of the pulse.

It is also useful to know that if we interpret the pulse shape $h(t)$ as the probability density of the random variable t the *characteristic function* of this process is by definition the integral

$$\Phi(\omega) = \int_{-\infty}^{+\infty} h(t) \cdot e^{j\omega t} dt \quad (4.4)$$

We see from Eq. (4.4), $\Phi(-\omega)$ is the Fourier transform of $h(t)$.

The function

$$\Psi(\omega) = \ln(\Phi(\omega)) \quad (4.5)$$

is the *second characteristic function* of t and is sometimes also called the *cumulant-generating function*. The cumulants λ_n of a random variable are by definition the derivatives

$$\lambda_n = \frac{1}{j^n} \left. \frac{\partial^n \Psi(\omega)}{\partial \omega^n} \right|_{\omega=0} \quad (4.6)$$

and are closely related to the distribution's moments [1].

Using Eq. (4.1) the cumulant (with index number zero)

$$\lambda_0 = \Psi(0) = \ln\left(\int_{-\infty}^{+\infty} h(t) dt\right) = \ln(A) \quad (4.7)$$

In case that $h(t)$ is really a probability density function it would be $A=1$ and consequently $\lambda_0=0$.

The first cumulant (with index number one) is the expected value:

$$\lambda_1 = \frac{1}{j} \cdot \frac{1}{\Phi(0)} \frac{\partial \Phi(0)}{\partial \omega} = \frac{1}{jA} \int_{-\infty}^{+\infty} jt \cdot h(t) dt = t_c \quad (4.8)$$

and corresponds to first order moment or (Eq.(4.2)) the central time t_c if we regard $h(t)$ as pulse shape.

The second and third cumulants are respectively the second and third central moments (the second central moment is the variance):

$$\lambda_2 = \sigma^2 \quad (4.9)$$

$$\lambda_3 = M_3 \quad (4.10)$$

The higher cumulants are neither moments nor central moments, but rather more complicated polynomial functions of the moments.

Expanding $\Psi(\omega)$ into a series near the origin and using the definition Eq. (4.6), we obtain

$$\Psi(\omega) = \lambda_0 + \lambda_1 j\omega + \frac{1}{2} \lambda_2 (j\omega)^2 + \frac{1}{3!} \lambda_3 (j\omega)^3 + \dots + \frac{1}{n!} \lambda_n (j\omega)^n + \dots \quad (4.11)$$

Because of the definition in Eq. (4.5) the characteristic function of the variable t is given by

$$\Phi(\omega) = \exp(\Psi(\omega)) \quad (4.12)$$

If $h(t)$ is the pulse response of the fiber its spectrum $H(\omega)$ and consequently the transfer function of the fiber is determined by substituting ω by $-\omega$ in Eq. (4.12) and we maintain using the Eqs. (4.7), (4.8), (4.9), and (4.10):

$$H(\omega) = \exp(\Psi(-\omega)) = \exp(\lambda_0) \cdot \exp\left[-j\omega\lambda_1 - \frac{\omega^2}{2}\lambda_2 + \frac{j\omega^3}{6}\lambda_3 \pm \dots\right]. \quad (4.13)$$

$$= A \cdot \exp\left[-j\omega t_c - \frac{\omega^2}{2}\sigma^2 + j\frac{\omega^3}{6}M_3 \pm \dots\right]$$

Thus, for a Gaussian shaped pulse response $h(t)$ all cumulants of higher order $\lambda_3=\lambda_4=\lambda_5=\dots=0$ being zero (all odd central moments M_3, M_5, \dots are zero) all terms in the exponent of Eq.(4.13) of third order and above are zero.

Consequently, to the extent that the impulse response of the POF can be regarded as Gaussian shaped insofar its transfer function $H_{POF}(f)$ can be approximated by a Gaussian characteristic too and the phase has to be linear.

5 Transfer Function dependent on POF-length

Assuming the Gaussian approach (following Eq. (4.13)) the transfer function for the POF can be approximated by

$$H(\omega) = A \cdot e^{\left[-j\omega t_c - \frac{\omega^2}{2}\sigma^2\right]} \quad (5.1)$$

with central time t_c dependent on the fiber length approximately $t_c = 4.97\text{ns/m} \cdot L_{POF}$ (L_{POF} =POF-length in m; refractive index of fiber core being $n_1=1.49$).

The relationship between the standard deviation σ and the electrical 3dB-bandwidth is given by:

$$\sigma = 0.132 / B_{3dB} \quad (5.2)$$

The relationship between the variables 20% to 80% rise time, electrical 3dB-bandwidth, and standard deviation is given by Eqs. (5.3) and (5.4).

$$t_{20-80\%} = 0.222 / B_{3dB} \quad (5.3)$$

$$t_{20-80\%} = 1.682 \cdot \sigma = 0.656 \cdot t_{10-90\%} \quad (5.4)$$

A variety of empirical expressions for modal dispersion have been developed. From practical experience it has been found that the bandwidth B_{3dB} in a link of length L_{POF} can be expressed to a reasonable approximation by the empirical relation

$$B_{3dB} = B_0 \cdot L_{POF}^{-q} \quad (5.5)$$

where the parameter q ranges between 0.5 and 1, and B_0 is the bandwidth for a fiber of 1m length.

Figure 5-1 shows the application of Eq. (5.5) for a polymer fiber (Luminous) exited by a launching aperture of AN=0.5 for a fiber length of 8m to 20m.

Thus, in case of launching aperture being AN=0.5 the length dependent transfer function of a polymer optical fiber can be approximated by

$$H_{POF}(f) = A \cdot \exp\left(-2(\pi\sigma f)^2\right) \cdot \exp(-j \cdot 2\pi f \tau L_{POF}) \quad (5.6)$$

with

$$A = 10^{\frac{\alpha \cdot L_{POF}}{10dB}} ; \alpha = \text{fiber loss in dB/m}$$

$$B_{3dB} = 1009 \cdot 10^6 \cdot L_{POF}^{-0.8747}$$

$$\sigma = 0.132/B_{3dB}$$

$$\tau = 4.97 \cdot 10^{-9} \text{ s/m}$$

insert L_{POF} in m

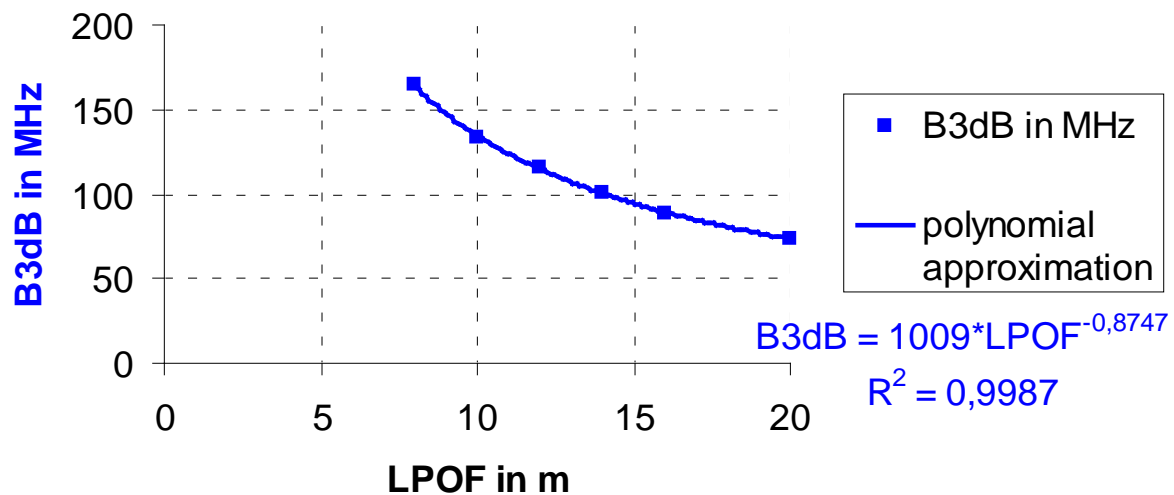


Figure 5-1: Measured bandwidth versus POF-length (Luminous) for launching AN=0.5 with polynomial curve fitting

The Figure 5-2 to Figure 5-7 show a very good agreement of the measured transfer functions for varies fiber lengths with the Gaussian approximation using Eq. (5.6) up to frequencies twice the bandwidth (fiber loss has been not taken into consideration).

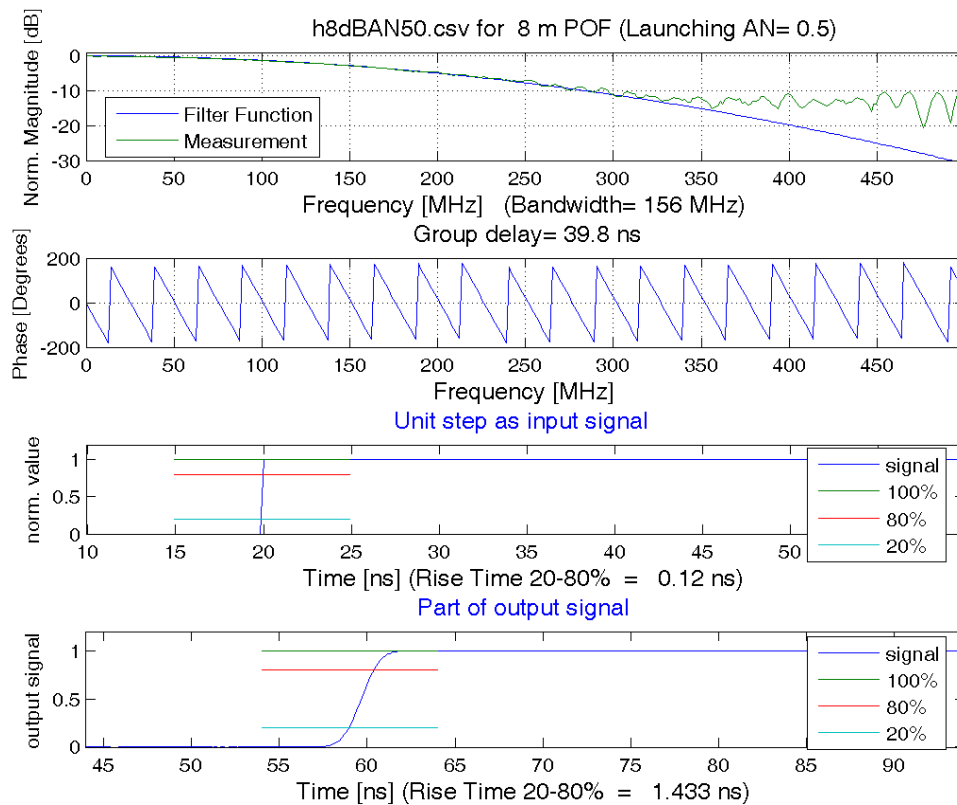


Figure 5-2: Comparing measured transfer function and Gaussian fit for 8m POF

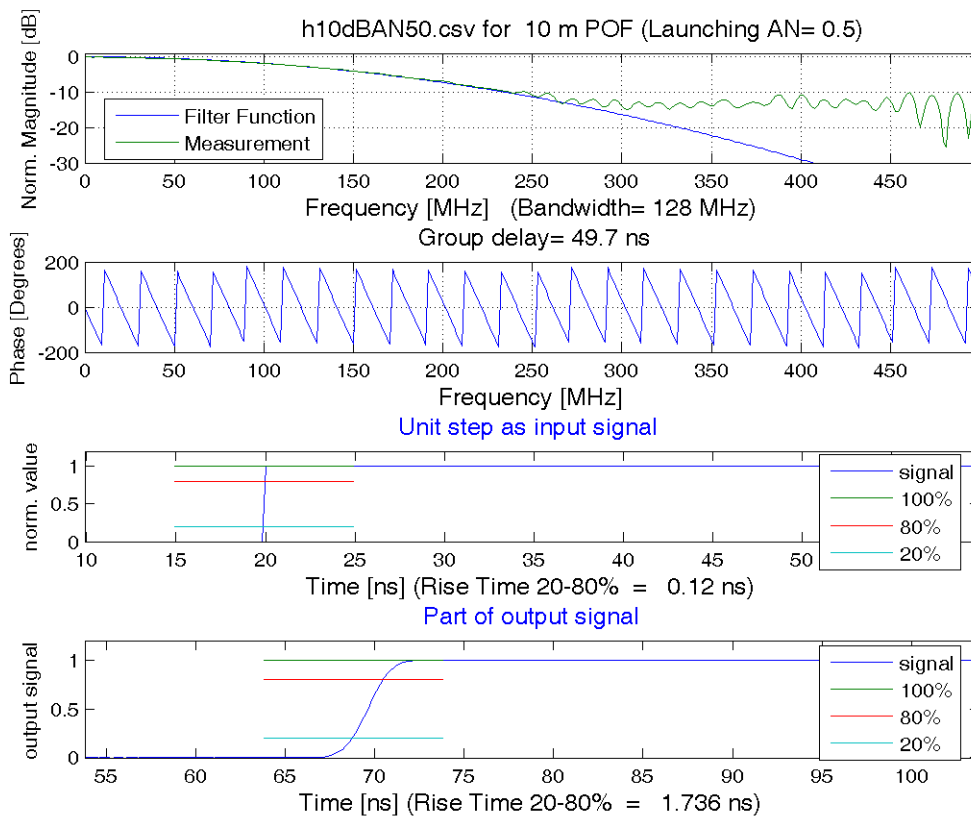


Figure 5-3: Comparing measured transfer function and Gaussian fit for 10m POF

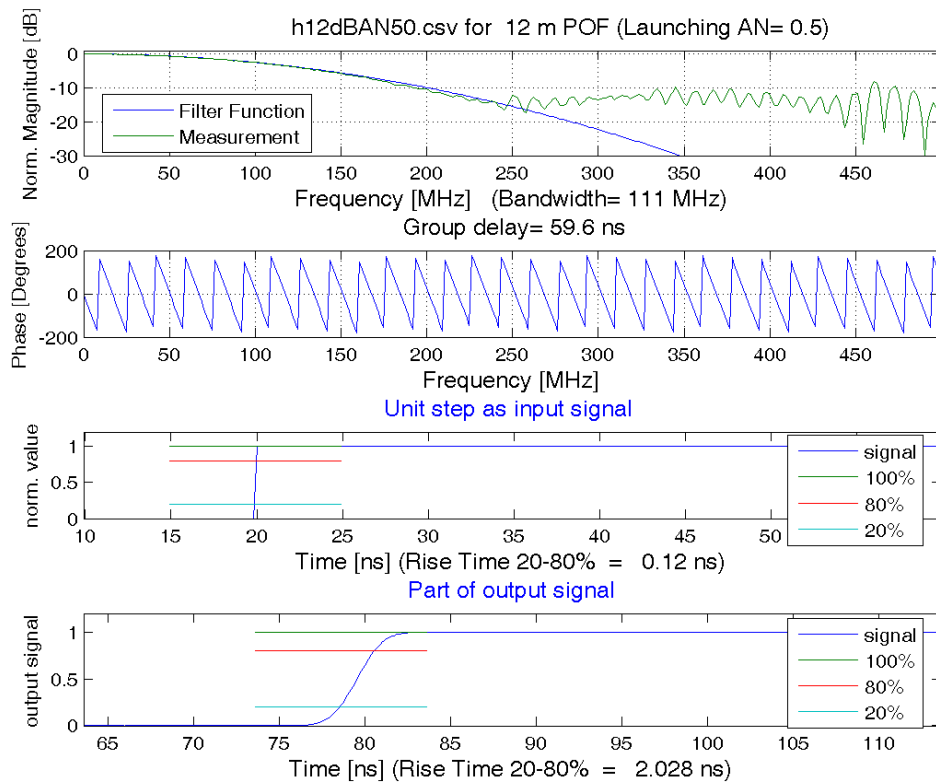


Figure 5-4: Comparing measured transfer function and Gaussian fit for 12m POF

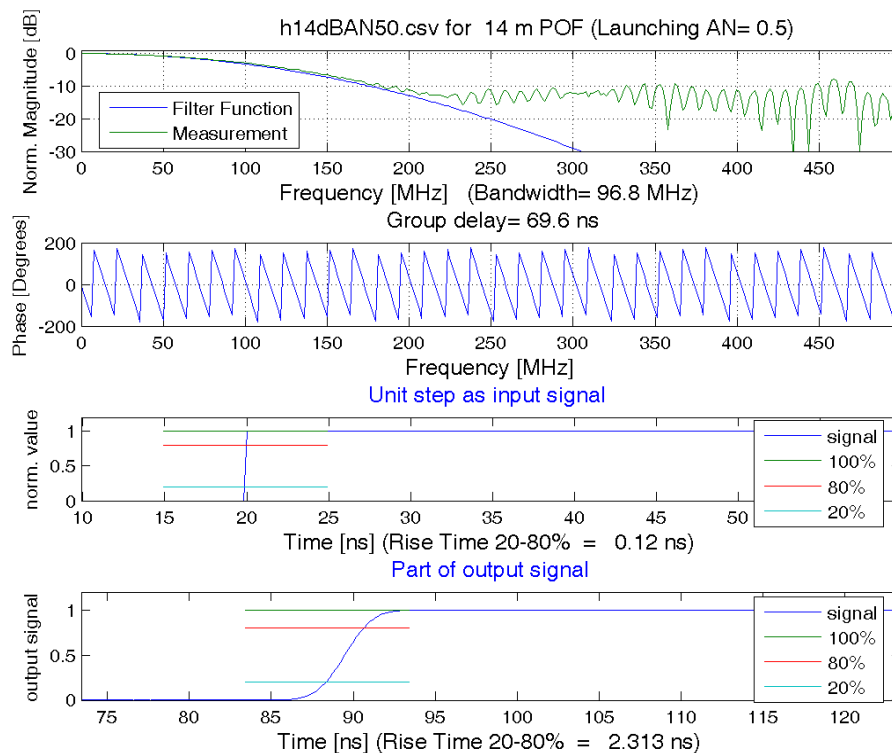


Figure 5-5: Comparing measured transfer function and Gaussian fit for 14m POF

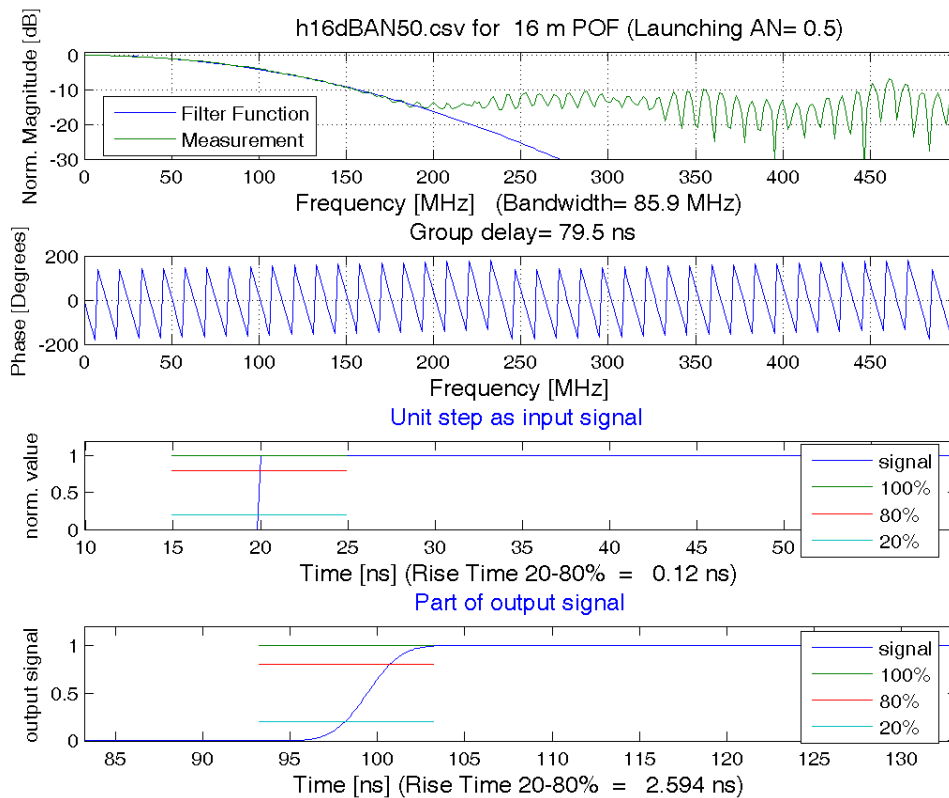


Figure 5-6: Comparing measured transfer function and Gaussian fit for 16m POF

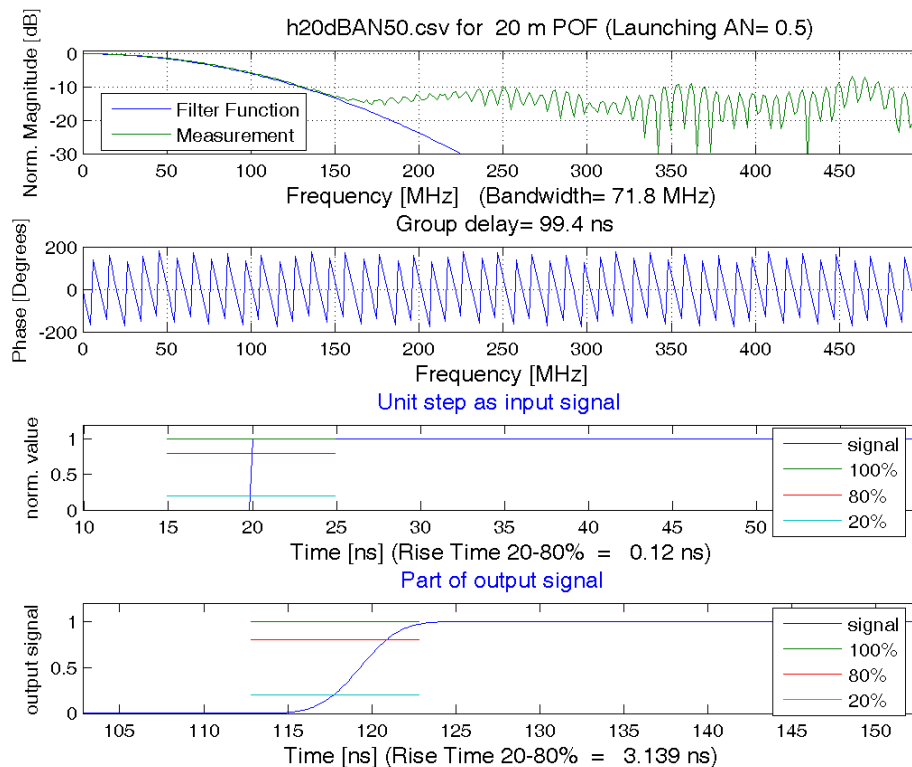


Figure 5-7: Comparing measured transfer function and Gaussian fit for 20m POF

Considering the ripple content in the measured transfer function that starts slightly above twice the bandwidth the expression to approximate this characteristic becomes significantly more complex. Additionally with respect to Eq. (5.5) and (5.6) the value of B_0 should be changed to $B_0=940$. The corresponding formula is given by:

$$\begin{aligned}
 B_{3dB} &= 940 \cdot 10^6 \cdot L_{POF}^{-0.8747} \\
 \sigma &= 0.132 / B_{3dB} \\
 f_0 &= 300 \cdot 10^6 \text{ Hz} \\
 A &= 10^{\frac{\alpha \cdot L_{POF}}{10 \text{ dB}}} ; \alpha = \text{fiber loss in dB/m} \\
 \tau &= 4.97 \cdot 10^{-9} \text{ s / m} \\
 &\text{insert } L_{POF} \text{ in m} \\
 H_{HF}(f) &= \frac{\frac{1}{2} \cdot (1 - \exp(-j4\pi f L_{POF} / f_0)) \cdot (1 - \exp(-j2\pi f / B_{3dB} / 80))}{(1 - 0.25 \cdot \exp(-j4\pi f L_{POF} / f_0))} \\
 H_{POF}(f) &= A \cdot \left\{ \exp(-2(\pi\sigma f)^2) + |H_{HF}(f)| \cdot \exp(-(f / 6 / B_{3dB})^2) \right\} \\
 &\quad \cdot \exp(-j \cdot 2\pi f \tau L_{POF})
 \end{aligned} \tag{5.7}$$

The following figures compare the measured transfer functions and the approximation using Eq.(5.7). The calculated step responses also use the approximation according to Eq.(5.7).

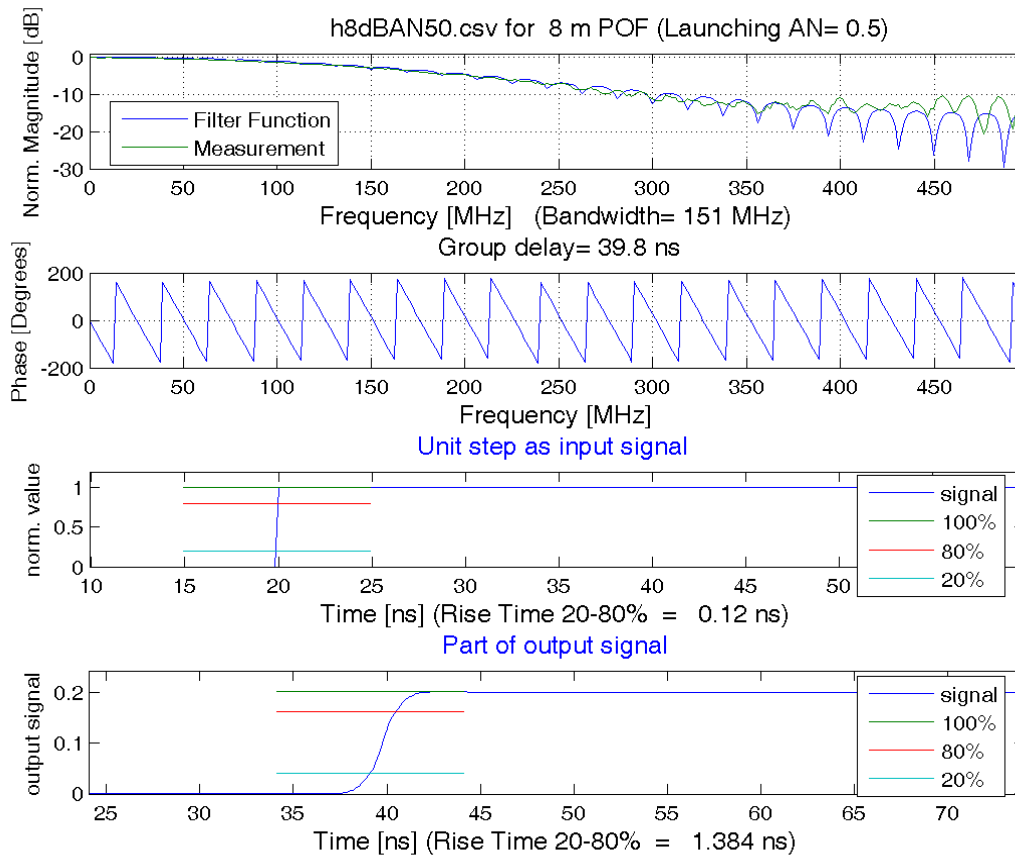


Figure 5-8: Comparing measured transfer function and Eq.(5.7) fit for 8m POF

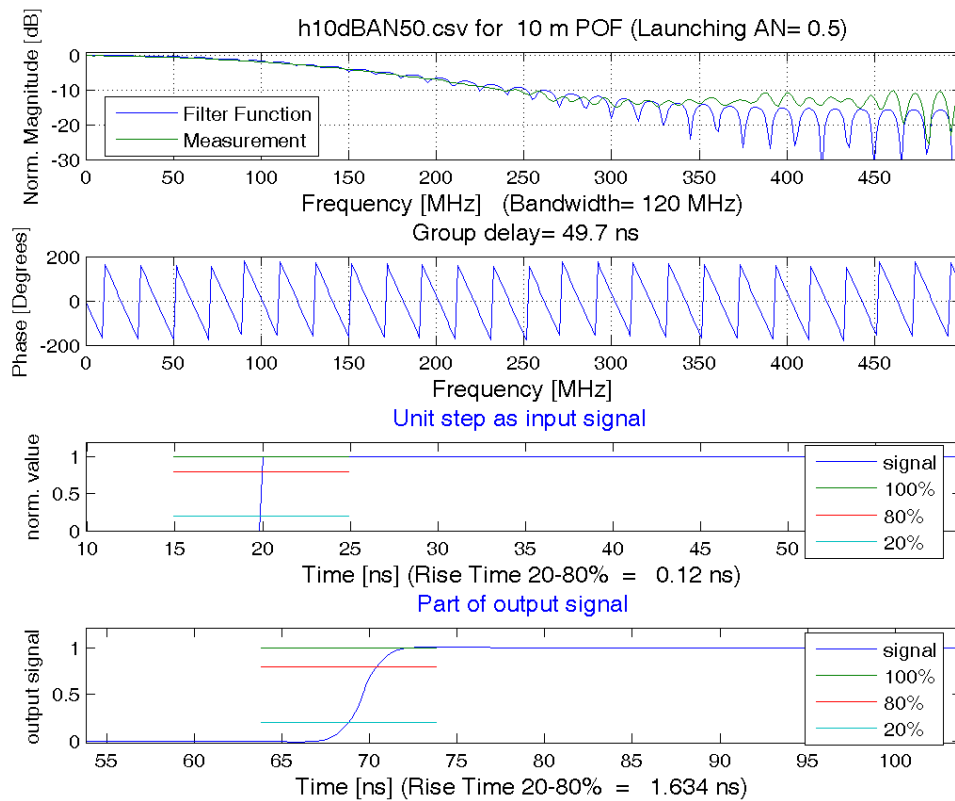


Figure 5-9: Comparing measured transfer function and Eq.(3.7) fit for 10m POF

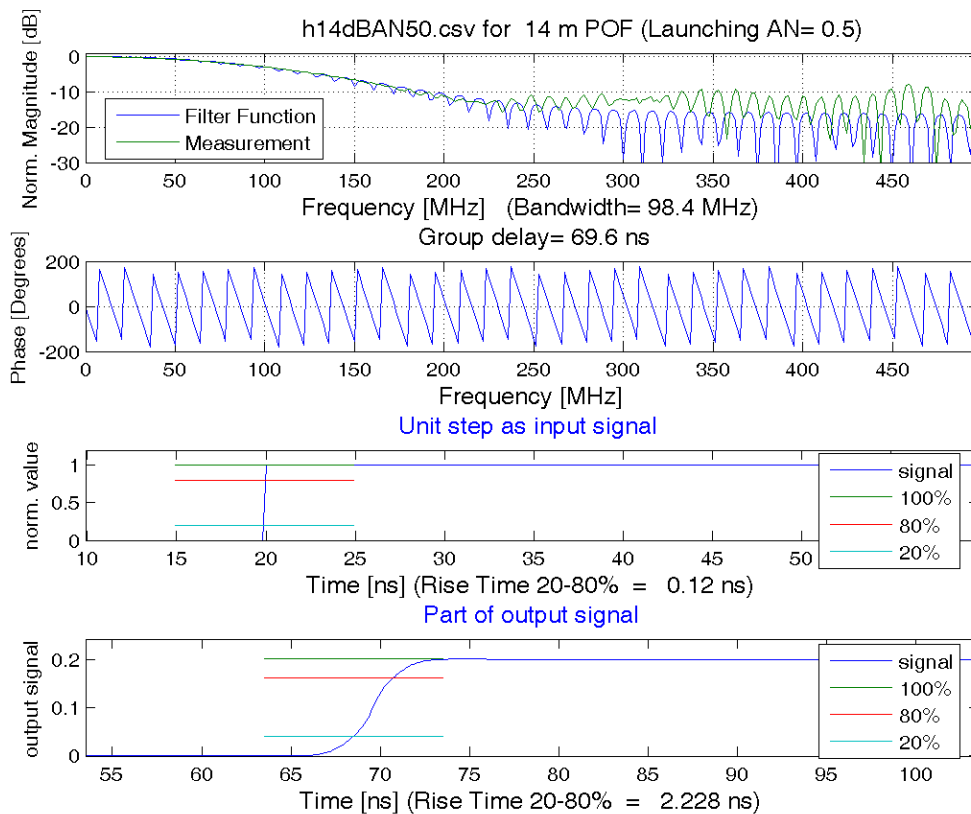


Figure 5-10: Comparing measured transfer function and Eq.(5.7) fit for 14m POF

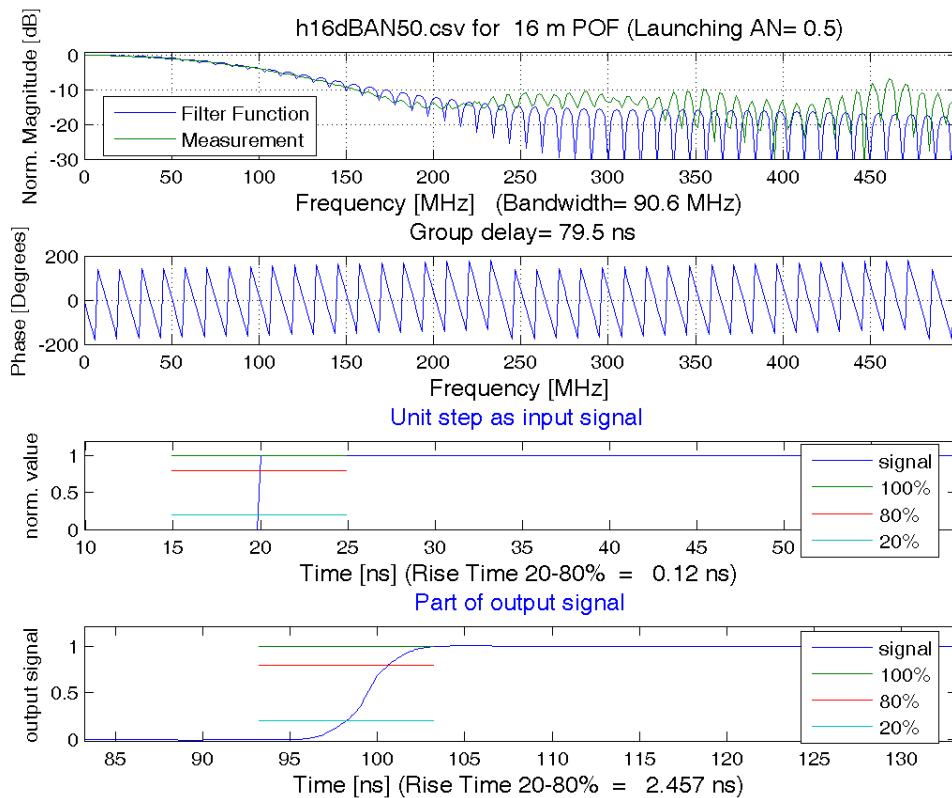


Figure 5-11: Comparing measured transfer function and Eq. (3.7) fit for 16m POF

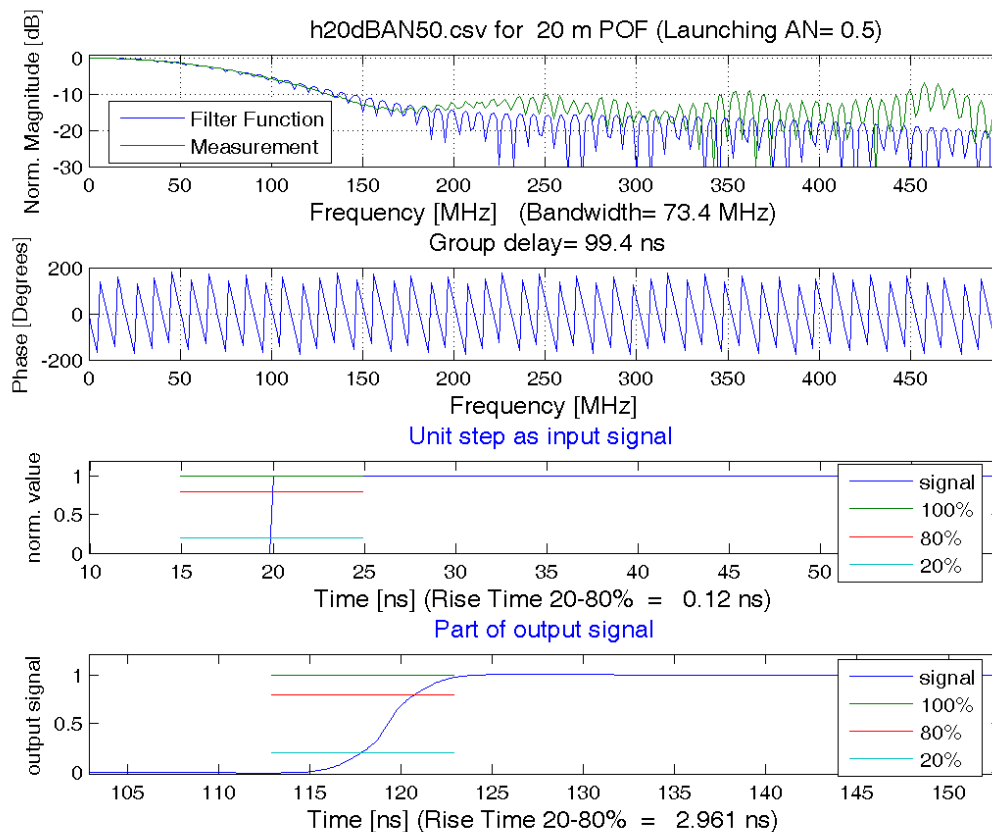


Figure 5-12: Comparing measured transfer function and Eq. (3.7) fit for 20m POF

6 Transfer Function dependent on Launching Aperture

Following the refraction law by Snellius the maximum angle Θ for total reflection at the core-cladding boundary is given by:

$$\cos \Theta = \frac{n_{\text{clad}}}{n_{\text{core}}} \quad (6.1)$$

According to a simple approach regarding only the meridional rays in the fiber core the difference in transition time τ_{Modal} between the longest ray path (the highest-order mode) and the shortest ray path (the fundamental mode) is obtained from ray tracing by:

$$\begin{aligned} \tau_{\text{Modal}} &= \frac{n_{\text{core}}}{c} L_{\text{POF}} \left(\frac{1}{\cos \Theta} - 1 \right) \\ &= \frac{n_{\text{core}}}{c} L_{\text{POF}} \cdot \frac{n_{\text{core}} - n_{\text{clad}}}{n_{\text{clad}}} \\ &= \frac{n_{\text{core}}^2}{c \cdot n_{\text{clad}}} L_{\text{POF}} \cdot \Delta \end{aligned} \quad (6.2)$$

with the index difference Δ defined by $n_{\text{clad}} = n_{\text{core}} \cdot (1 - \Delta)$. Because Δ is much less than 1 the numerical aperture AN of the fiber is approximated by

$$AN = n_{\text{core}} \cdot \sqrt{2\Delta} \quad (6.3)$$

Using Eq. (6.3) and Eq. (6.2) we calculate

$$\tau_{\text{Modal}} = \frac{L_{\text{POF}}}{2c \cdot n_{\text{clad}}} \cdot AN^2 \quad (6.4)$$

Although this approach neglects any kind of mode coupling and thus might lead to an underestimation of fiber bandwidth it suggests itself that the pulse broadening arising from τ_{Modal} is proportional to AN^2 . Thus, the bandwidth is proportional to $1/AN^2$.

In respect of Eq. (6.4) it is supposed that in Eq. (5.5) B_0 can be approximated by a polynomial function second order of $(1/AN)$. The parameter q equals 1 in the case of no mode coupling and with an increasing amount of mode coupling it decreases down to $q=0.5$ in case of dynamic equilibrium mode mixing [2]. Figure 6-1 and Eq. (6.5) include expressions for a polynomial approximation for both parameters that can be used to fit the measured bandwidth of varies polymer fiber lengths and under different launching aperture conditions, respectively.

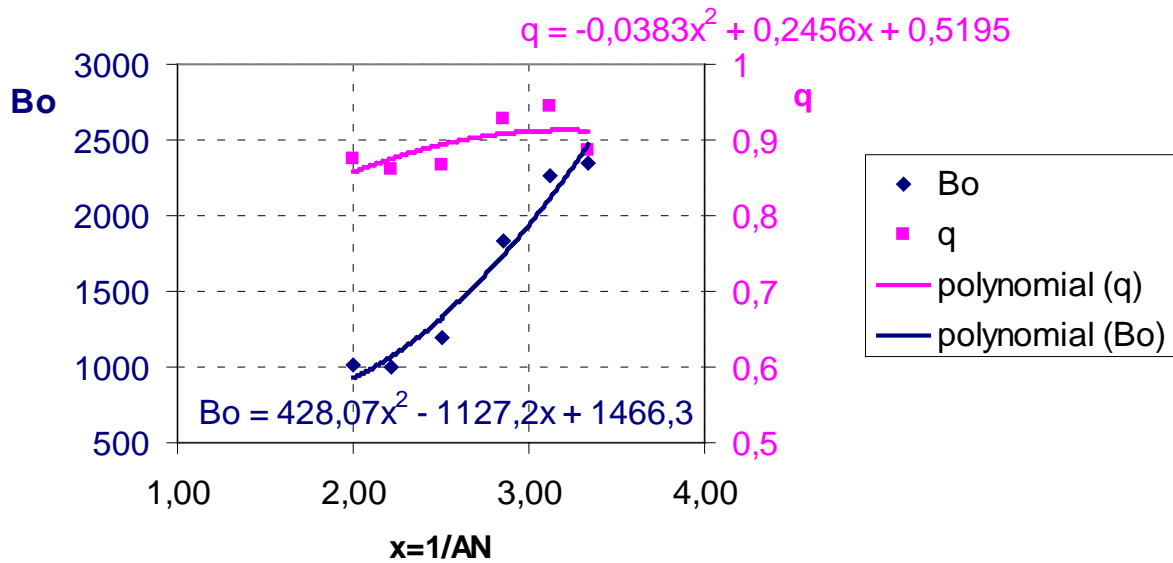


Figure 6-1: Influence of numerical aperture on bandwidth parameters with polynomial approximations

Figure 6-2 compares measured bandwidth data and calculated values versus launching aperture for different POF-lengths. The calculation uses

$$B_{3dB} = B_0 \cdot L_{POF}^{-q} \quad (6.5)$$

with

$$B_0 = 428.07/AN^2 - 1127.2/AN + 1466.3$$

$$q = -0.0383/AN^2 + 0.2456/AN + 0.5195$$

Using B_{3dB} according to Eq. (6.5) together with Eq. (5.6) we calculate the Gaussian approximation for the transfer function dependent on POF-length and launching aperture as:

$$\begin{aligned} \sigma &= 0.132/B_{3dB} \\ H_{POF}(f) &= A \cdot \exp\left(-2(\pi\sigma f)^2\right) \cdot \exp(-j \cdot 2\pi f \tau L_{POF}) \\ \tau &= 4.97 \cdot 10^{-9} \text{ s/m} \\ A &= 10^{\frac{\alpha \cdot L_{POF}}{10 \text{ dB}}} ; \alpha = \text{fiber loss in dB/m} \\ &\text{insert } L_{POF} \text{ in m} \end{aligned} \quad (6.6)$$

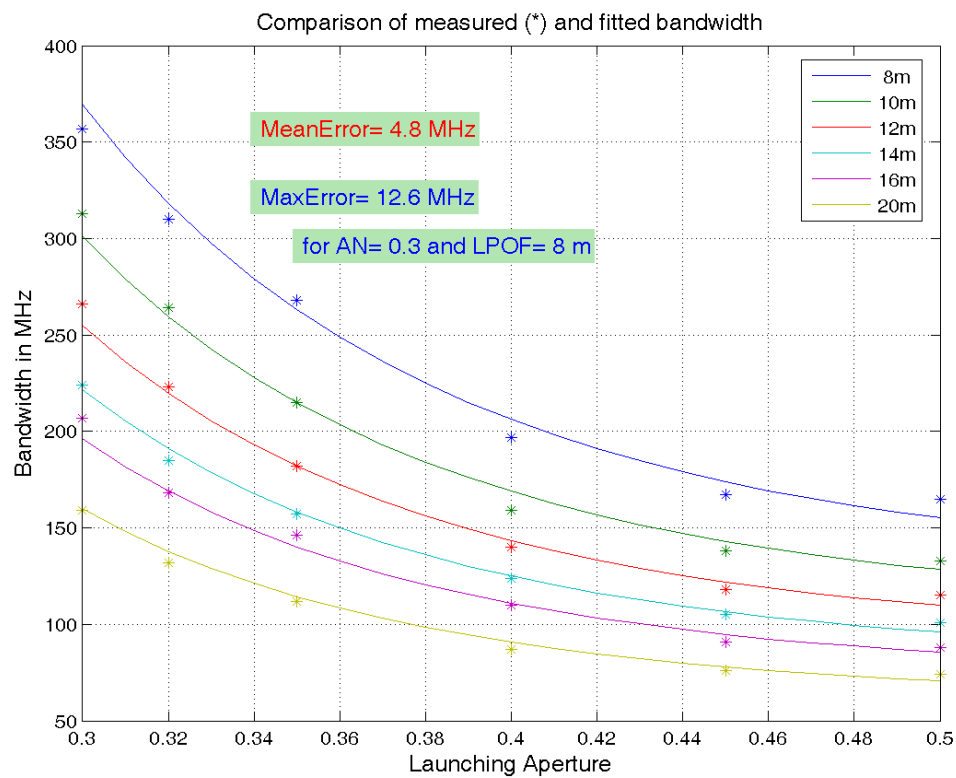


Figure 6-2: Electrical 3dB-bandwidth versus launching aperture - measurement and approximation – various POF length

Measured electrical bandwidth in MHz							Calculated electrical bandwidth in MHz using Gaussian transfer function						
AN\ LPOF in m	8	10	12	14	16	20	AN\ LPOF in m	8	10	12	14	16	20
0,30	357	313	266	224	207	159	0,30	370	301	255	222	196	160
0,32	310	264	223	185	168	132	0,32	318	260	220	191	169	138
0,35	268	215	182	157	146	112	0,35	263	215	182	158	140	114
0,40	197	159	140	124	110	87	0,40	206	169	144	125	111	91
0,45	167	138	118	105	91	76	0,45	174	143	122	107	95	78
0,50	165	133	115	101	88	74	0,50	156	128	111	97	86	72

Table 6.1: Values for measured and calculated bandwidths

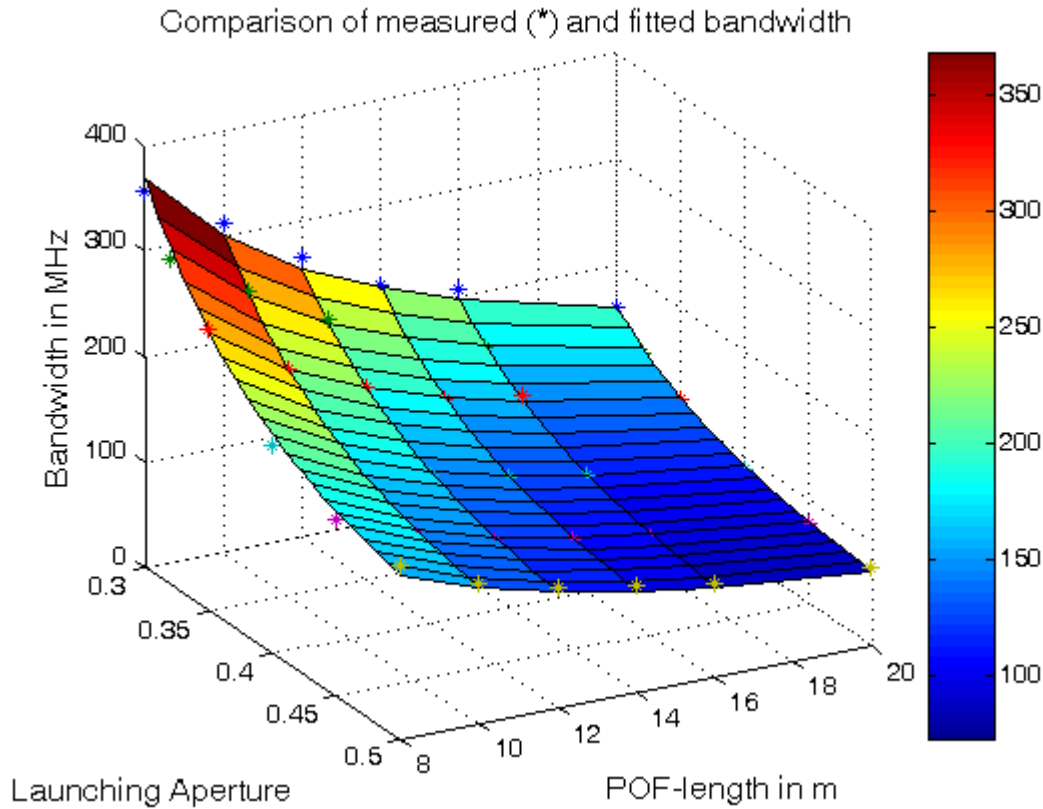


Figure 6-3: Three-dimensional view of 3dB-bandwidth B_{3dB} according to Eq.(6.5)

In order to upgrade Eq. (5.7) by the launching aperture dependency Eq. (6.5) can be used as well, however, with a correction factor for the B_{3dB} value according to

$$B_{3dB} = 0.9316 \cdot B_0 \cdot L_{POF}^{-q} \quad (6.7)$$

$$B_0 = 428.07/AN^2 - 1127.2/AN + 1466.3$$

$$q = -0.0383/AN^2 + 0.2456/AN + 0.5195$$

Use only in combination with Eq. (5.7) !

7 Using model equations

Given the signal $s_{P2}(t)$ emitted by the light source, the application of Eq. (6.5) and Eq. (6.6) offers the possibility to predict the signal shape $s_{P3}(t)$ at the fiber end (SP3) by calculation. This requires the evaluation of the input signal's spectrum $S_{P2}(f)$ by Fourier transforming $s_{P2}(t)$ (e.g. using DFT). The signal spectrum at $S_{P3}(f)$ at fiber end is then given by

$$S_{P3}(f) = S_{P2}(f) \cdot H_{POF}(f) \quad (7.1)$$

The fiber's output signal $s_{P3}(t)$ is determined by the reverse Fourier transformation of $S_{P3}(f)$ and thus can be used for further investigations like eye diagram calculations, rise time statistics etc.

For example we assume a POF-length of 15m, a launching aperture of AN=0.5 and for simplicity we neglect the fiber's attenuation ($\alpha=0\text{dB/m}$) and group delay ($\tau=0\text{s}$). For the fiber input signal $s_{P2}(t)$ three examples of different MOST150 input data pattern (SIM slow, SIM ov, and SIM tst) were used. These examples do not cover all MOST150 input signal variants (e.g. jitter).

The results of the application of the POF's transfer function are shown in the appendix (chapter 10).

It should be stated explicitly, the calculations exhibit that the fiber influences duty cycle in case of "SIM ov" and "SIM tst". The fiber also adds ISI and increases transition time of rising and falling edges of the signal due to bandwidth limitation.

The $B_{-3\text{dB}}$ bandwidth values given in the figures of chapter 10 refer to the electrical 3dB-bandwidth of the fiber. Using the Eq. (5.3) the corresponding pulse response rise time $t_{20-80\%}$ may be evaluated. For the underlying data ($L_{\text{POF}}=15\text{m}$, launching AN=0.5) it is $t_{20-80\%} = t_{\text{POF}}=2.45\text{ns}$. It must be emphasized that adding the square t_{POF}^2 to the square of the input signal's rise time t_{SP2}^2 results only in the square of the output signal's rise time t_{SP3}^2 insofar the pulse shape of the input signal is Gaussian. The more the signal shape differs from the Gaussian shape, i.e. the signal pulse exhibits significant moments of order greater than 2, the worse the following equation is fulfilled:

$$t_{\text{SP3}}^2 = t_{\text{SP2}}^2 + t_{\text{POF}}^2 \quad (7.2)$$

As a consequence of Eq. (4.13) being a generic representation of a system's transfer function only the variances of pulse responses sum up to the aggregate variance of pulse response of concatenated systems. Thus, regarding the fiber as the transmission system, only the variances of input pulse and pulse response sum up to the variance of output pulse. Because of the input signals "SIM ov" and "SIM tst" exhibit a quite asymmetric shape of each pulse, i.e. are significantly different from Gaussian shape, the application of Eq. (7.2) is strictly not possible and might lead to errors.

8 Conclusion

In consideration of Figure 5-2 to Figure 5-7 the Gaussian approach using Eq. (5.6) is a very good approximation for the measured transfer functions of polymer fibers of 8m up to 20m in lengths. Eq. (5.6) matches the transfer characteristic sufficiently up to frequencies twice the bandwidth for a launching aperture AN=0.5.

Considering varies AN-values as launching aperture the use of Eq. (6.5) and Eq. (6.6) is recommended. For this the degree of accuracy and the range of validation are demonstrated in Figure 6-2, Figure 6-3 and Table 6.1.

Given the signal data pattern, the signal shape at the fiber output can be evaluated dependent on fiber length and launching aperture. Furthermore, the influence of the transmitter and receiver transfer characteristic can be considered if the corresponding transfer functions of these components are identified.

9 References

- [1] Athanasios Papoulis: *Probability, Random Variables, and Stochastic Processes*, McGraw-Hill, 1985, Chap. 5-5
- [2] S. Geckeler: *Pulse broadening in optical fibers with mode mixing*, App. Optics Vol 18, No. 13, July 1979

10 Appendix: Evaluation results for 15m POF and launching aperture 0.5

For three examples (SIM slow, SIM ov, and SIM tst) the following figures include POF transfer function, input signal (dotted line) and calculated output signal (solid line), rise and fall time determinations, and eye diagrams of input and output signal. In chapter 10.5 a MATLAB (version 7.0.1) script shows how to implement the simulation using Fast-Fourier-Transformation.

10.1 SIM slow

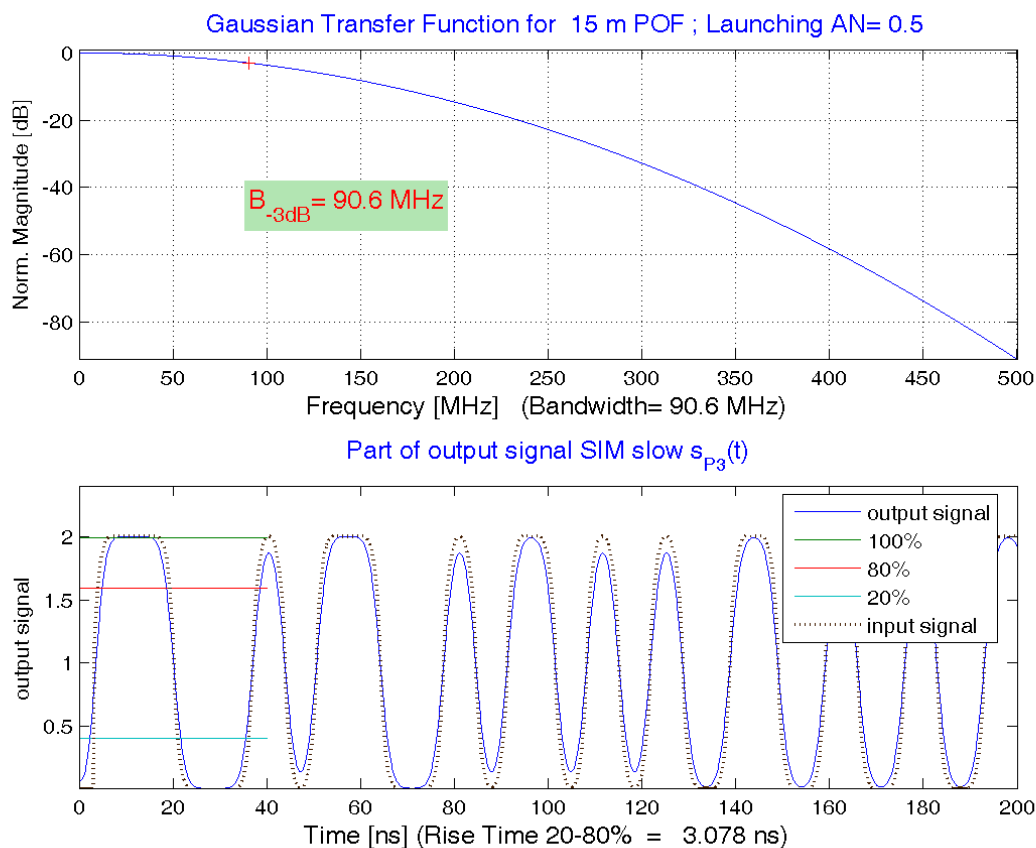


Figure 10-1: Transfer function and simulated output signal; input signal without overshoot

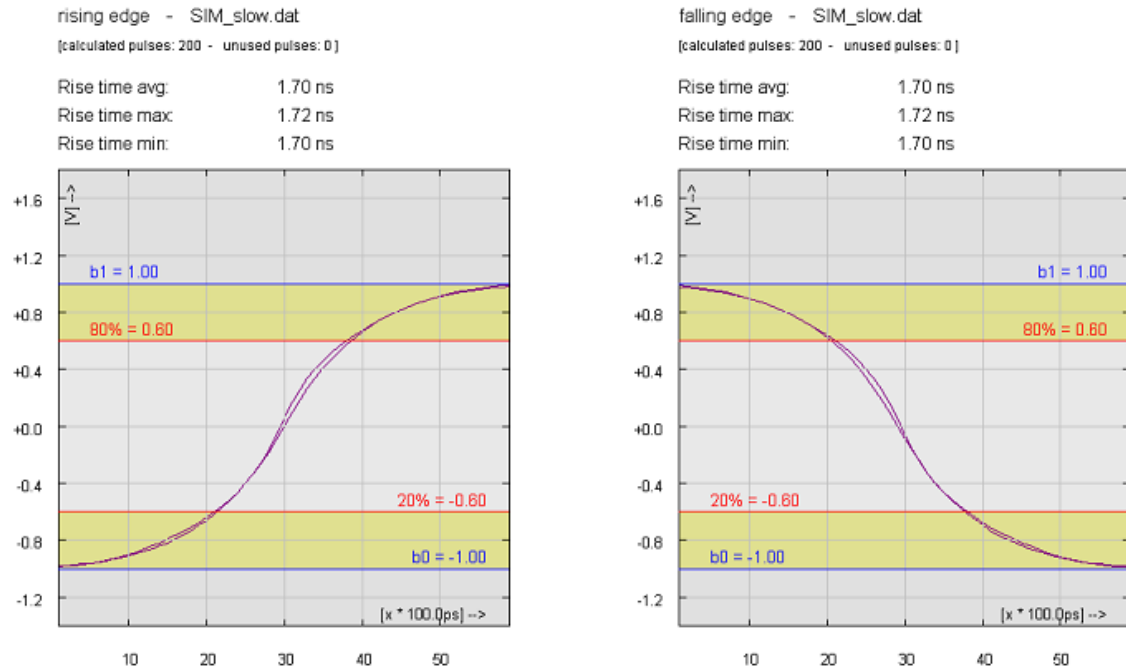


Figure 10-2: Rise and fall time of input signal SIM slow (SP2)

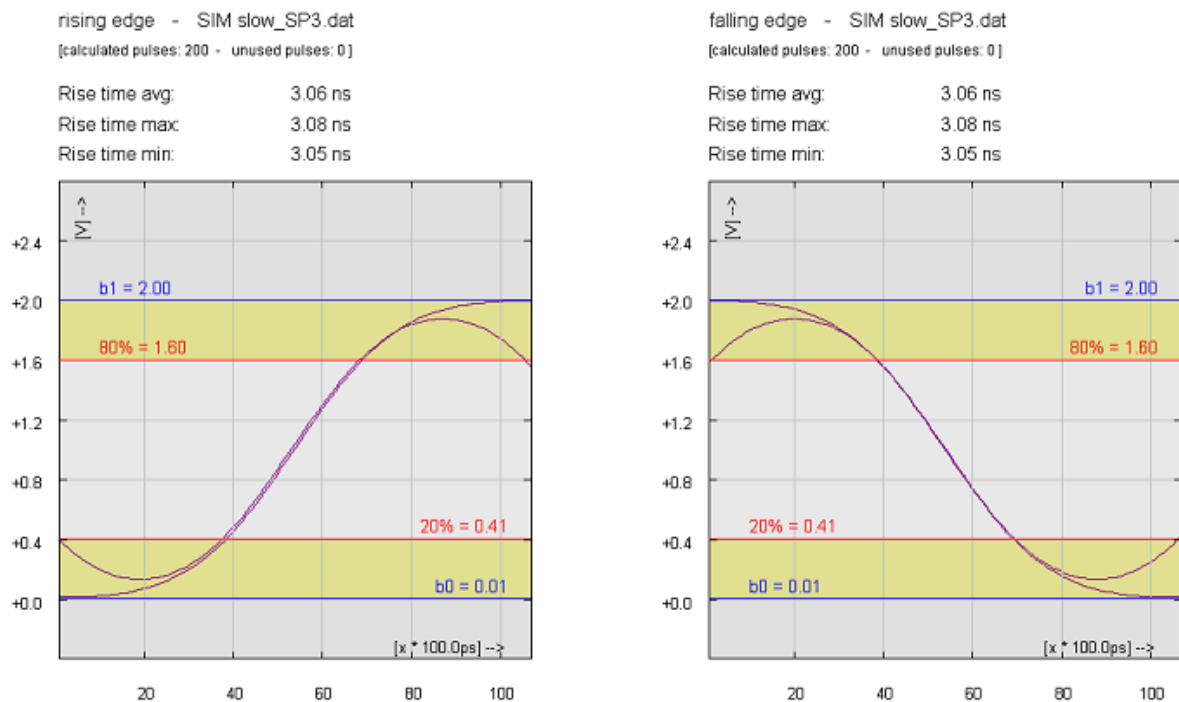


Figure 10-3: Rise and fall time of output signal SIM slow_SP3

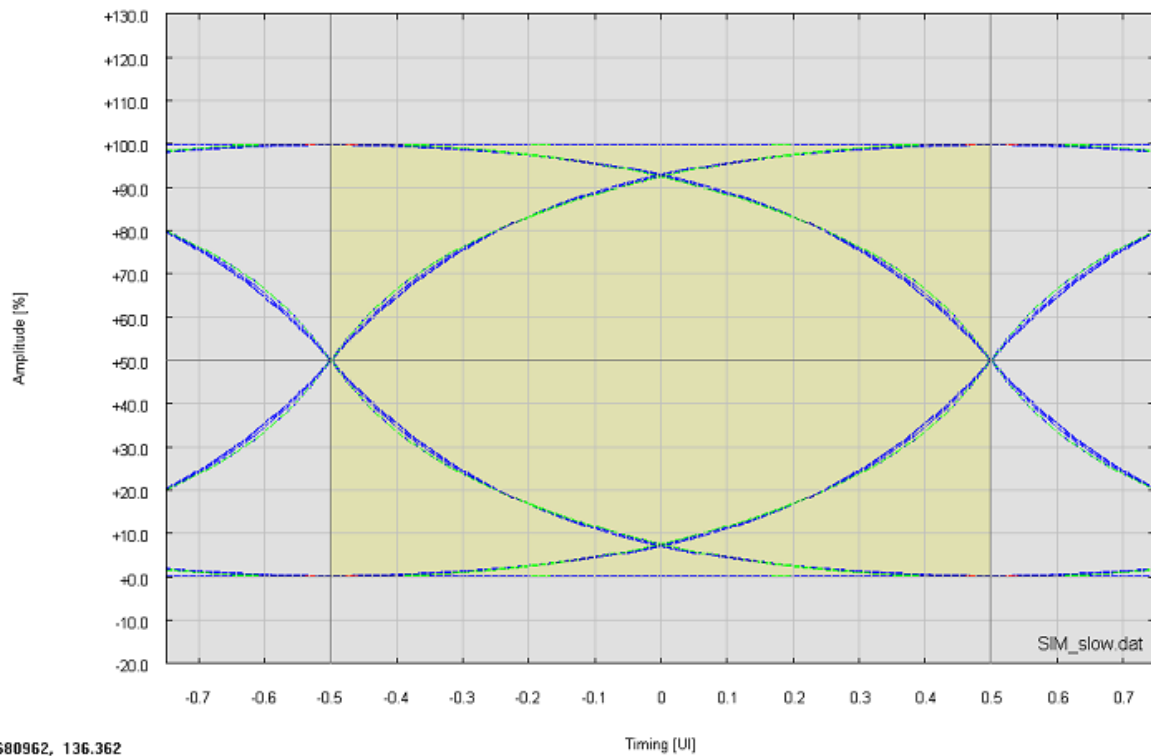


Figure 10-4: Eye diagram of input signal SIM slow (SP2)

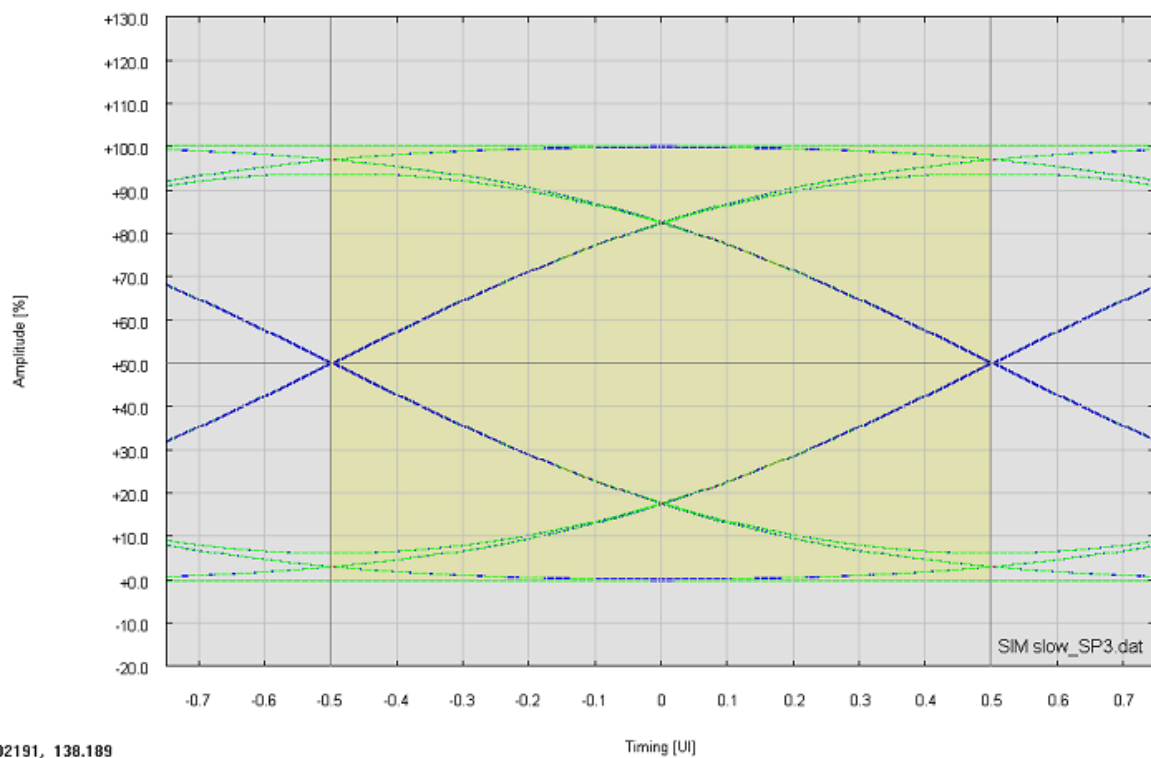


Figure 10-5: Eye diagram of output signal SIM slow_SP3

10.2 SIM ov

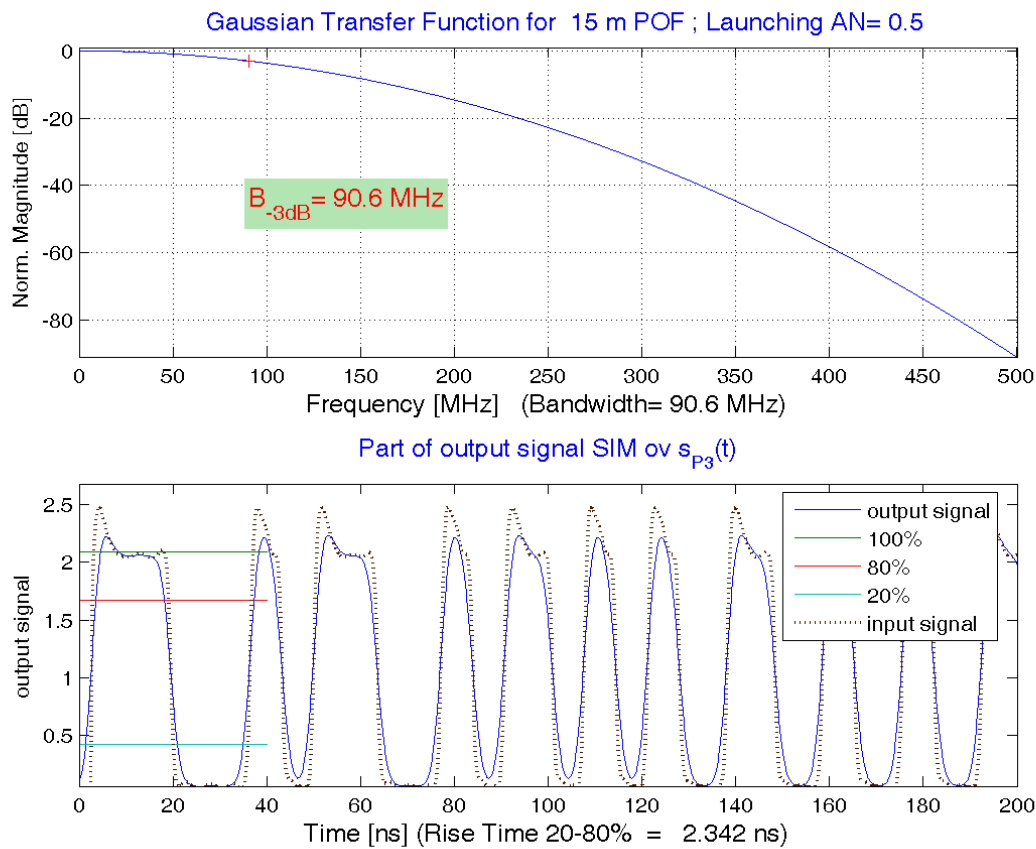


Figure 10-6: Transfer function and simulated output signal; input signal with overshoot

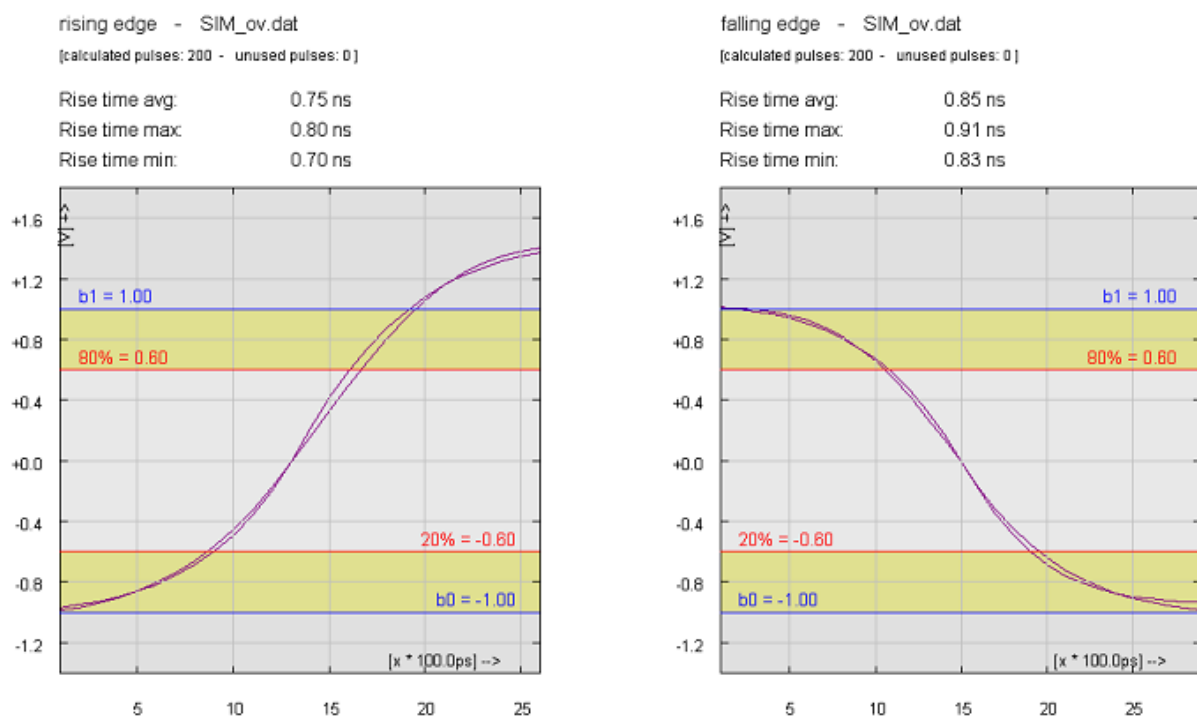
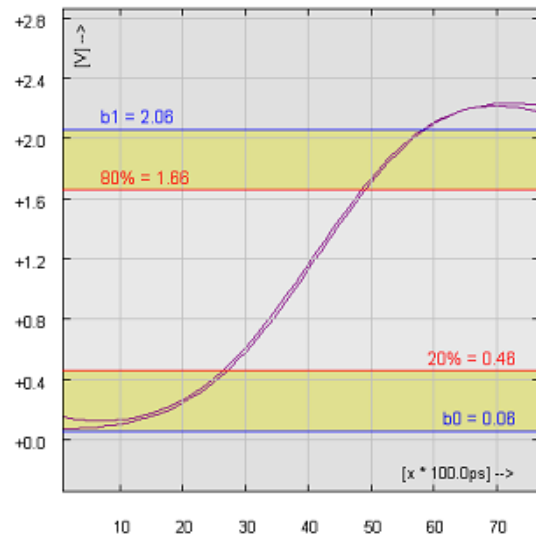


Figure 10-7: Rise and fall time of input signal SIM ov (SP2)

rising edge - SIM ov_SP3.dat
(calculated pulses: 200 - unused pulses: 0)

Rise time avg: 2.21 ns
Rise time max: 2.21 ns
Rise time min: 2.19 ns



falling edge - SIM ov_SP3.dat
(calculated pulses: 200 - unused pulses: 0)

Rise time avg: 2.59 ns
Rise time max: 2.64 ns
Rise time min: 2.52 ns

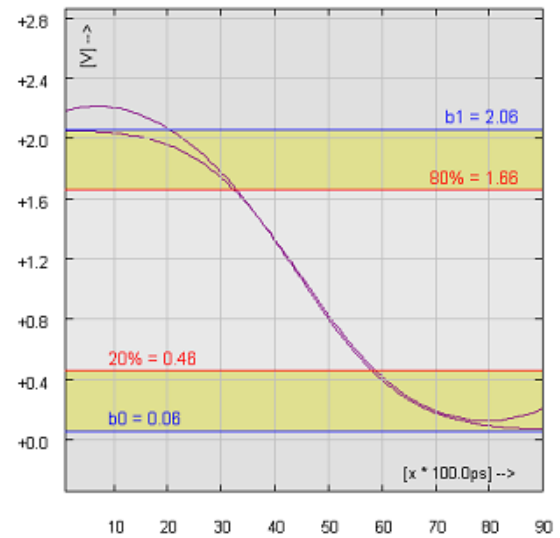
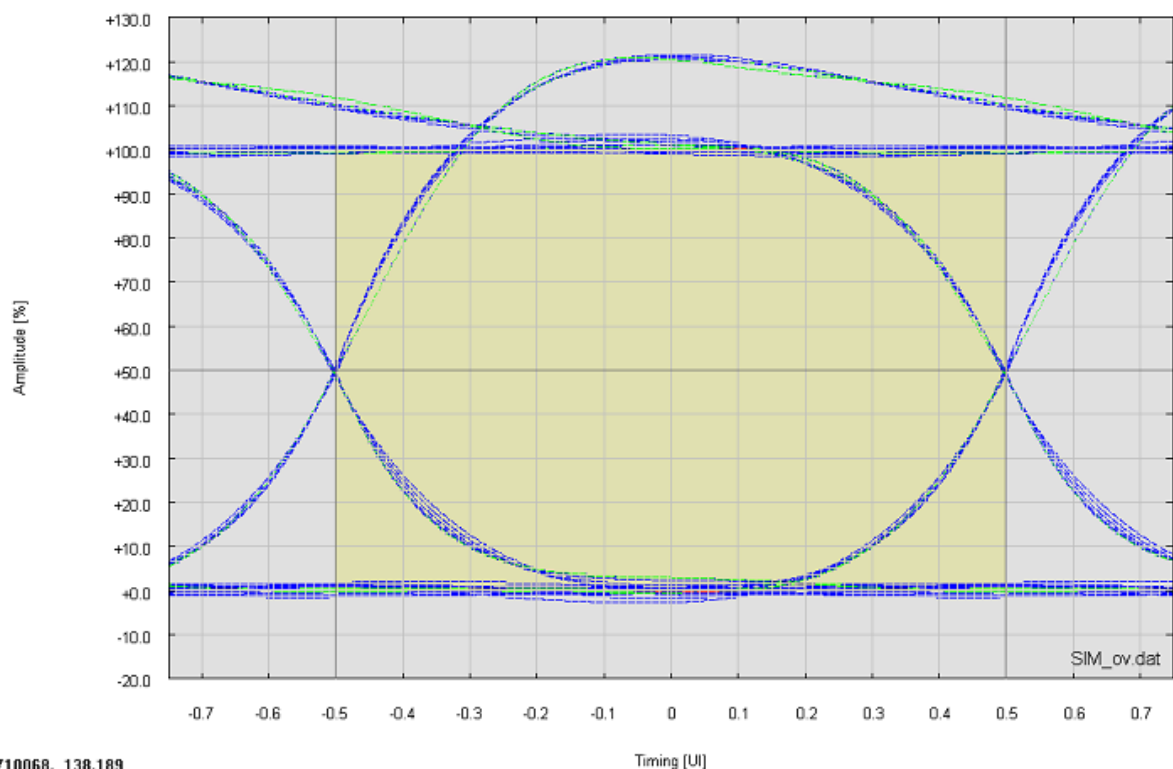


Figure 10-8: Rise and fall time of output signal SIM ov_SP3



-0.710068, 138.189

Figure 10-9: Eye diagram of input signal SIM ov (SP2)

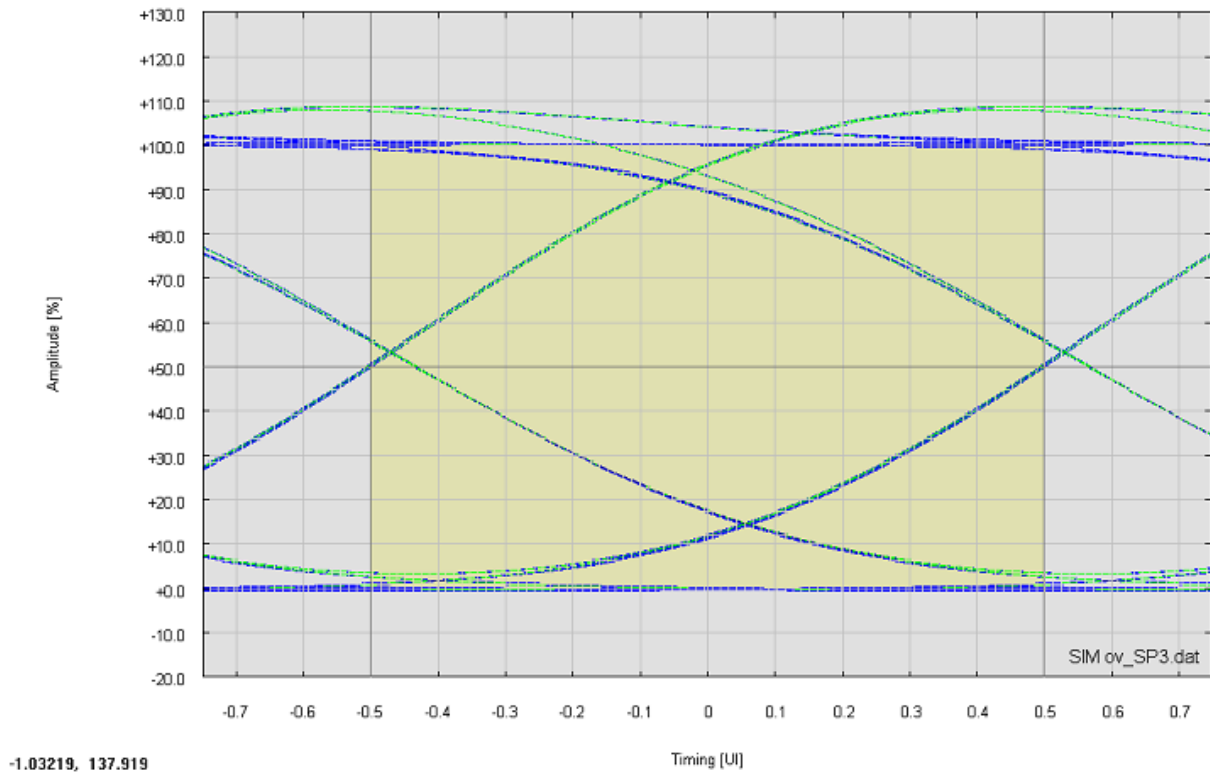


Figure 10-10: Eye diagram of output signal SIM ov_SP3

10.3 SIM tst

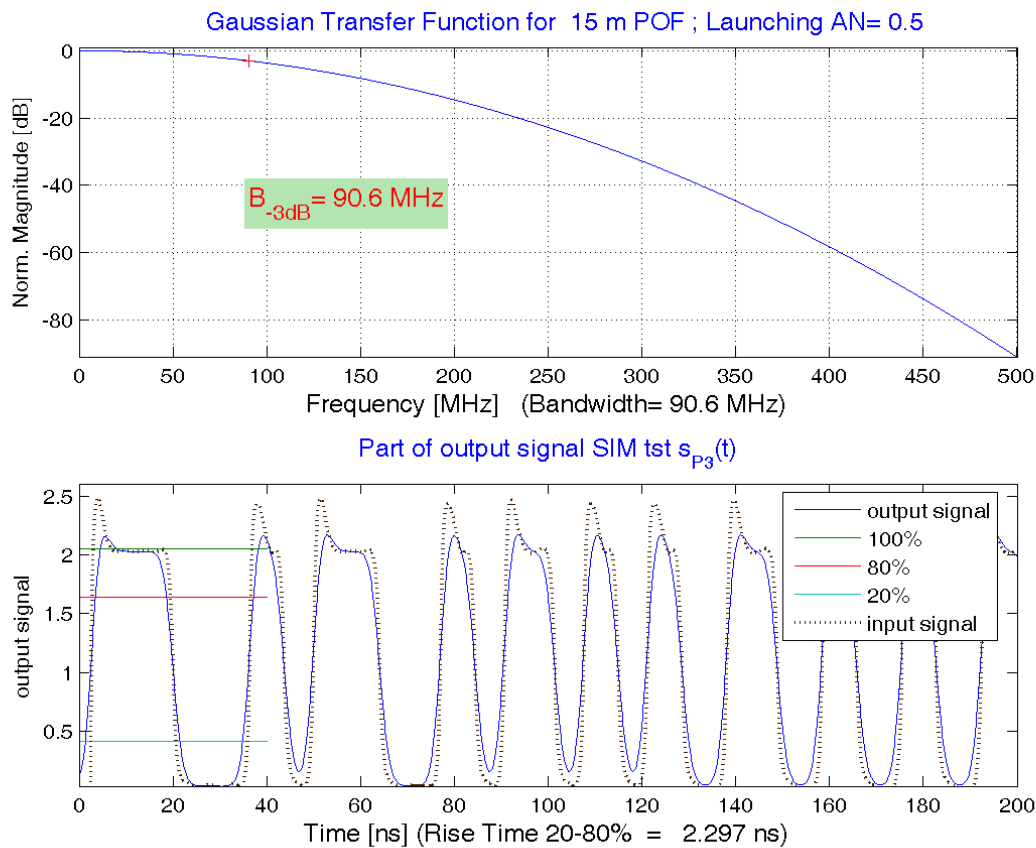


Figure 10-11: Transfer function and simulated output signal; input signal with overshoot and deteriorated duty cycle

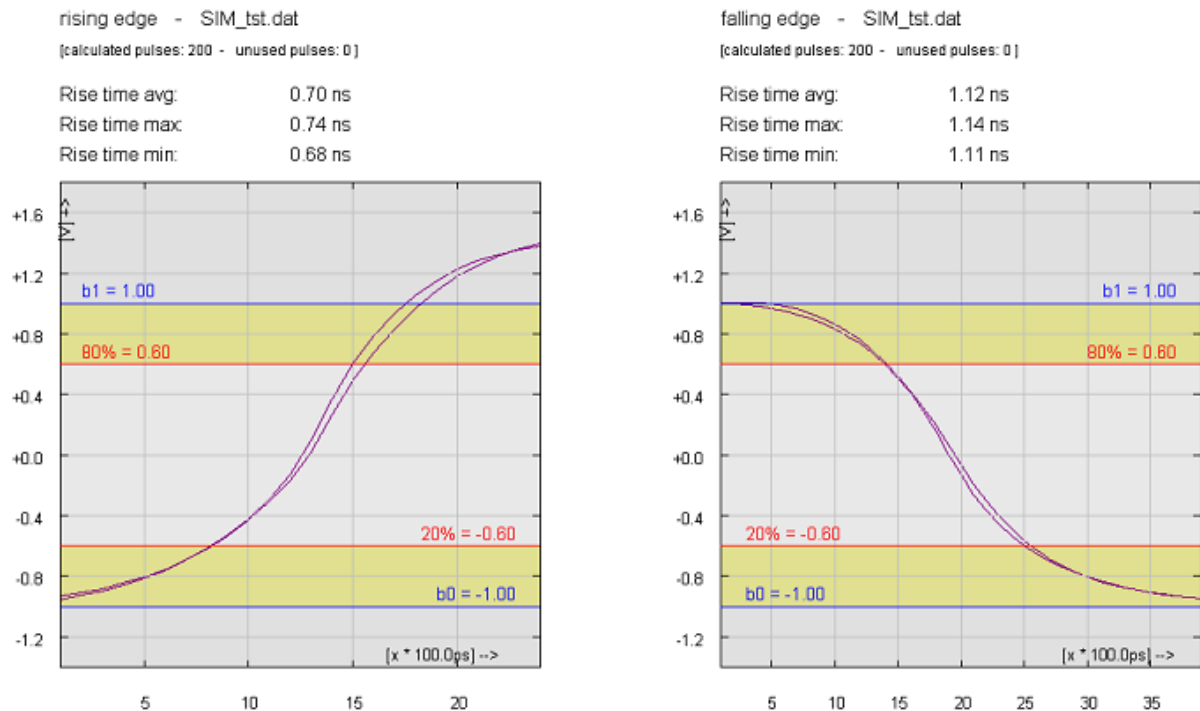


Figure 10-12: Rise and fall time of input signal SIM tst (SP2)

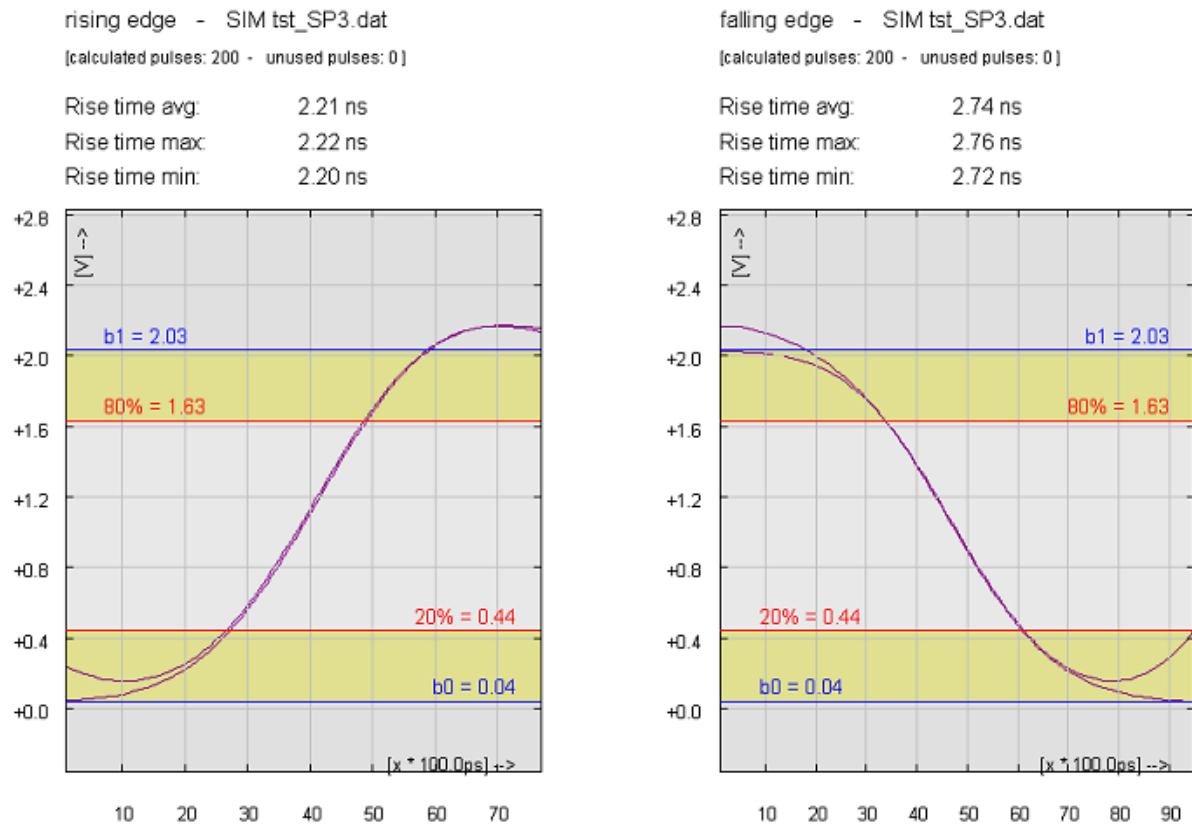


Figure 10-13: Rise and fall time of output signal SIM tst_SP3

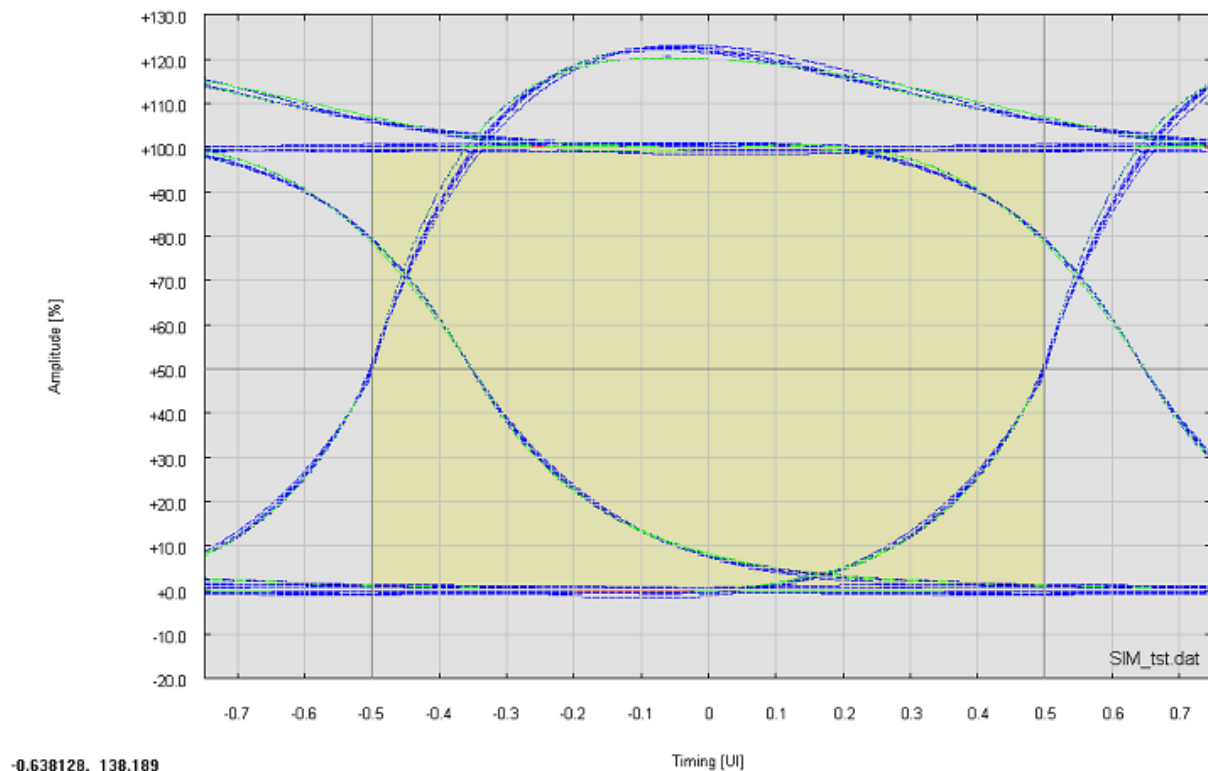


Figure 10-14: Eye diagram of input signal SIM tst (SP2)

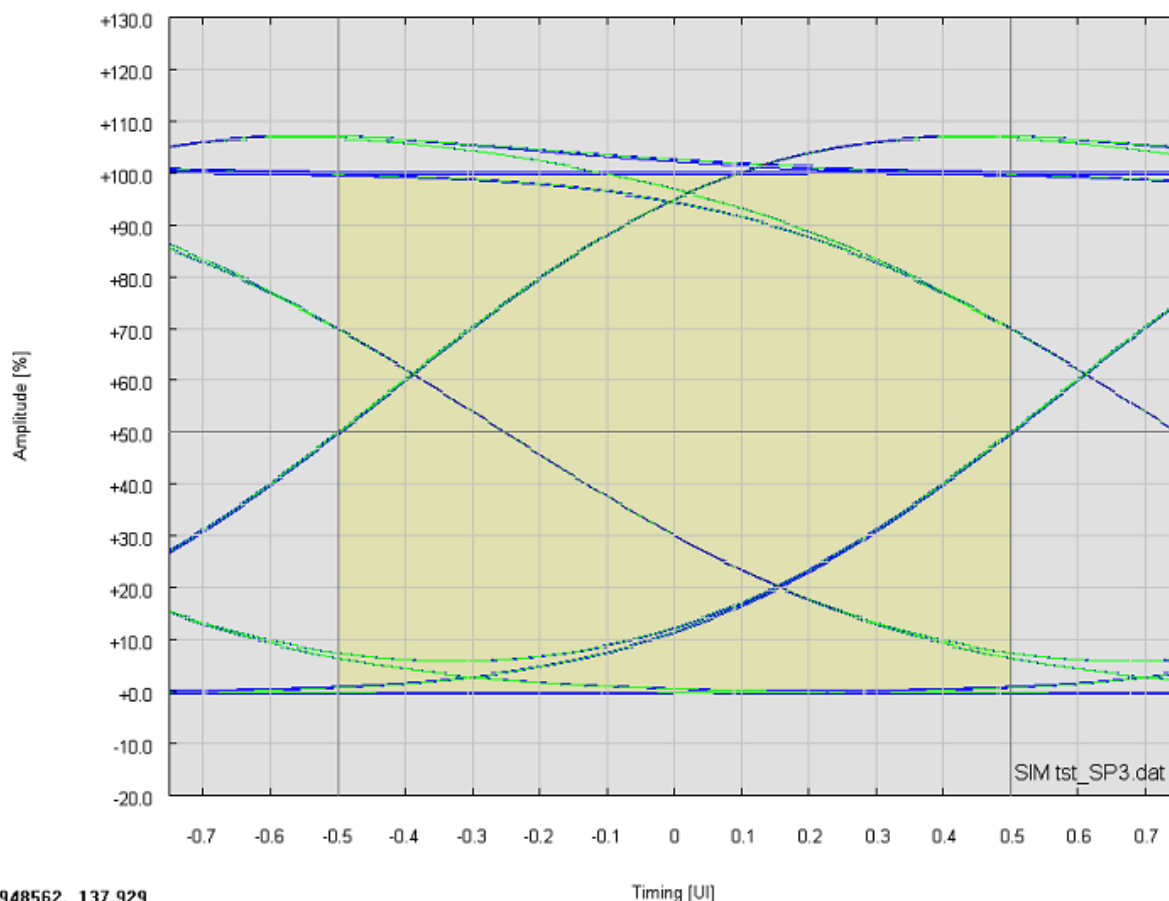


Figure 10-15: Eye diagram of output signal SIM tst_SP3

10.4 A set of rules for calculation

- *Remind periodicity of DFT*

It has been mentioned already that the signal at SP3 is calculated by Fourier transforming the input signal at SP2. Therefore a DFT is used. Being aware of the periodic nature of DFT it has to be taken into consideration that the DFT views both the time domain and the frequency domain as periodic. This can be inconvenient if the signal is not periodic. Nevertheless, if we use DFT, we have to conform with the DFT's view of the world.

- *Avoid time domain aliasing*

The time domain periodicity can be thought of as the right side of the acquired signal wraps around and connects to its left side. The most serious consequence of that is time domain aliasing. Due to bandwidth limitations the selected frequencies might be deleted or changed in amplitude or phase. These changes in the frequency domain can create a time domain signal that is too long to fit into the original period. Thus, the signal spills from one period to the adjacent. Because of the time domain is regarded as circular this new location already contains an existing signal, resulting in a loss of information. In order to avoid this time domain aliasing, a sufficient prolongation of the time interval by padding with zeros before and after the original input signal is recommended.

- *Flip spectrum*

Periodicity in the frequency domain behaves similar, but is more complicated. If we use N samples in the time domain the frequency spectrum within which the transfer function has to be evaluated is viewed as being composed of $N/2+1$ samples spread between 0 and 0.5 of the sampling rate f_s ($0.5 \cdot f_s = \text{Nyquist frequency}$). The key feature is that the frequency spectrum between 0 and $0.5 \cdot f_s = N/2 \cdot df$ appears to have a mirror image of frequencies that run between $0.5 \cdot f_s + df$ and $1 \cdot f_s - df$, where df is the step size in the frequency domain. This mirror image of frequencies is different insofar as the magnitude is flipped left-to-right, i.e. the magnitude $|H(0.5 \cdot f_s + df)| = |H(0.5 \cdot f_s - df)|$, $|H(0.5 \cdot f_s + 2df)| =$

$|H(0.5 \cdot f_s - 2df)|, \dots, \text{and } |H(0.5 \cdot f_s + (N/2 - 1)df)| = |H(0.5 \cdot f_s - (N/2 - 1)df)| = |H(df)|$. Notice that samples 0 and $N/2$ do not have a matching point in this duplication scheme. In terms of sample numbers, this makes the length of the frequency domain period equal to N , the same as in the time domain. For completeness, the phase of the spectrum is flipped left-to-right in the same manner and additionally changed in sign.

- *Consider Gibbs effect*

Frequently the original signal (at SP2) has truncated ends in the time domain. This usually leads to a discontinuity between the first and last sample, since the DFT views the time domain as periodic. In case that because of bandwidth limitations by the transfer function only some of the frequencies are used in the reconstruction, i.e. evaluation of signal at SP3, each edge shows overshoot and ringing. In other words, a truncation of the higher frequencies, results in overshoot and ringing at the edges in the time domain. Exactly at the discontinuity the value of the reconstructed signal converges to the midpoint of the step. This all is known as the Gibbs effect. By duality, to truncate the ends of the time domain signal, this distorts the edges in the frequency domain. As a consequence of all that, it is recommended to exclude the start and end of the signal at SP3 (first and last bit of the data pattern) for the signal characterization.

[illegible]


```
scrsz = get(0,'ScreenSize');
figure('Position',[1 scrsz(4)/2 scrsz(3)/1.2 scrsz(4)/1.2],...
      'Name',['Transmission of ' num2str(LPOF) ' m
POF'], 'nextplot', 'replace')
n1=1; n2=2000;
plot(t(n1:n2)*1e9,sp3(n1:n2));
    ylabel('output signal sp3(t)'), grid on,ylim([1.2*min(sp3)
1.2*max(sp3)])
    xlabel(['Time [ns]' ],'fontSize',12), grid off, xlim([t(n1)*1e9
t(n2)*1e9]);

%===== Output data to file =====
if length(Sfile)>0
    ipoint=findstr(Sfile,'.')->1;
    if ipoint else iblank=findstr(Sfile,' ')-1; ipoint=iblank(1);end
    dlmwrite([Sfile(1:ipoint) ' SP3.dat'], sp3');
end
```

11 Appendix: Automated Determination of Worst-Case Scenarios for the MOST Optical Physical Layer Specification Point 3

11.1 Introduction

For automated determination of worst-case scenarios for different parameter sets, a program based on MATLAB was developed. The software generates separate pulse shapes for rising and falling edges where the full tolerance range given by the MOST physical layer specification is utilized. These edges are combined to a single signal by using valid MOST patterns, coded in DC Adaptive Coding (DCA). Then the impact due to the transmission media is simulated (using filter algorithm shown in 10.5). The use of complete MOST frames guarantees that low frequencies are also included in the calculation. Afterwards the SP3 results are stored for visualization and analysis. These steps are iterated until the desired parameter coverage or cross-coverage is reached. The coverage is determined based on parameters for describing the pulse shapes of falling and rising edges.

11.2 SP3 Input Pattern Calculation

All patterns are generated using normalized amplitude and normalized time-scale. The amplitude is based on the steady state high- and low-level of the optical signals ("B₁", "B₀"). A specific method for achieving these parameters is given in the MOST Specification. Amplitude value 1 represents steady state "B₁"; an additional overshoot up to 1.4 is permitted. Amplitude 0 represents steady state "B₀", which doesn't necessarily mean zero. A small bias level is possible; a limitation is given by the parameter "extinction ratio". Time-scale is defined in Unit-Intervals (UI), derived from the network bit rate. Due to the coding scheme, the shortest pulse width is 2 UI. There are further pulse types with pulse length up to 6UI. The SP3 input pattern calculation is divided into three main steps. These steps are described in detail in the following three sections.

11.2.1 Rising and Falling Edge Generation

The generated transitions represent pulse shapes of 2 UI length. Rising edges start with amplitude 0 and end with amplitude 1, falling edges start with 1 and end with amplitude level 0.

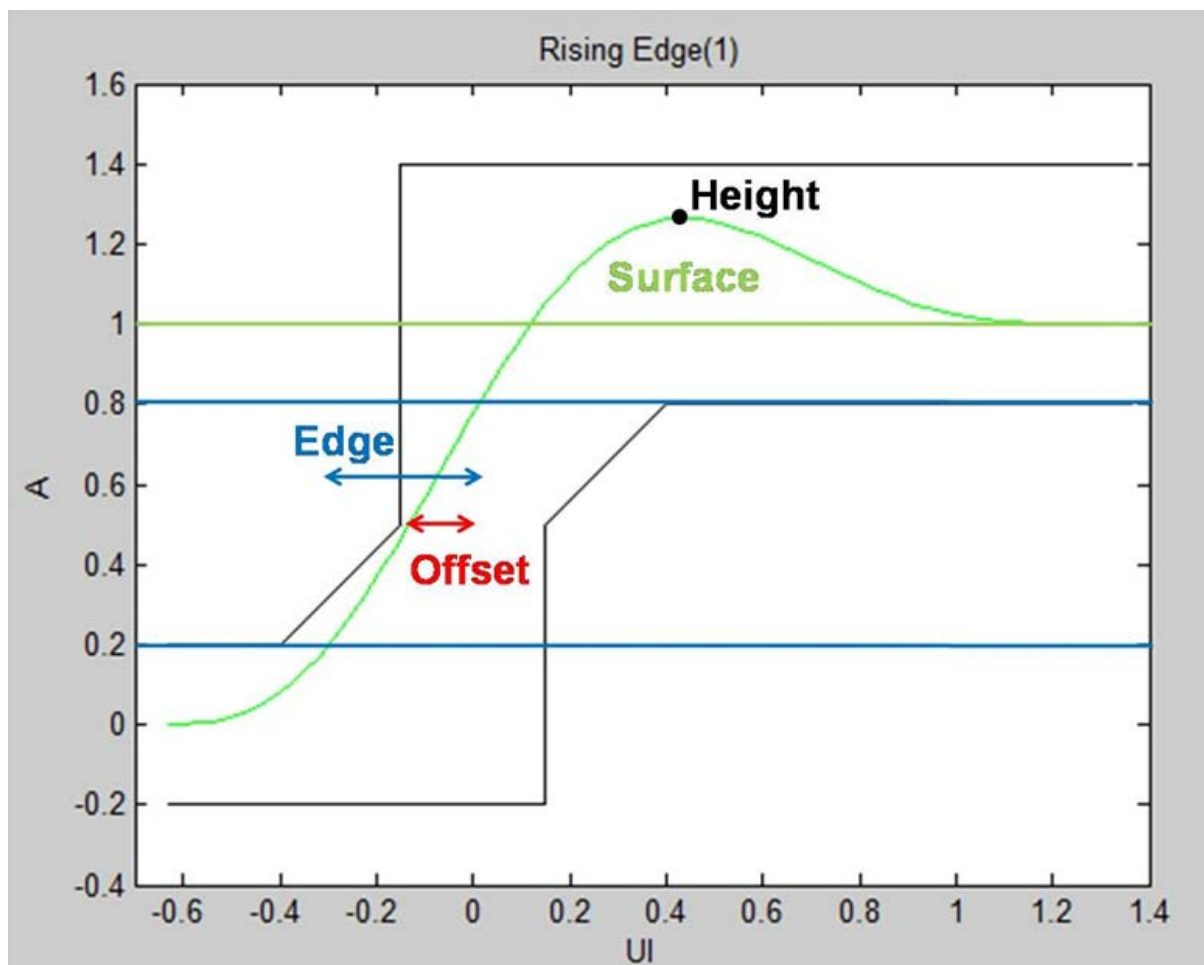


Figure 11-1: Pattern parameter

A rising and a falling edge is described by four parameters. These parameters are **Edge**, **Surface**, **Offset** and **Depth** for the falling edge and **Height** for the rising edge. Before generating an edge the minimum and maximum values of these parameters can be defined, to generate edges with special properties.

- **Edge:** Transition time between 20% and 80% of the normalized amplitude.
- **Surface:** Accumulated power within the surface over or under the normalized amplitude.
- **Offset:** Time deviation between transition and zero point on the time scale measured at amplitude level 0.5.
- **Depth, Height:** Peak-Amplitude of the generated rising or falling edge pattern.

For generating pulse shapes, coordinates at start and end of the curve are fixed, while sample points in between are generated randomly. In order to control the process of generating random coordinates, boxes are defined wherein one random coordinate per trial is generated. Then curves are fitted through the sample points using Matlab Polyfit in which basic polynomial and spline interpolation is possible. The timing resolution for was chosen with 30 samples/UI. The method of limiting the degree of freedom by introducing the boxes helps to avoid unrealistic pulse shapes and allows an adaptation to the needs of the chosen fit-algorithm. The random ranges for polynomial interpolation are shown in Fig 3. After a calculation run, the pulse shape is checked for consistency with the SP2-requirements and the user defined parameter range. If all constraints are matched, the pulse shape is accepted or else the algorithm runs through 10,000 trials.

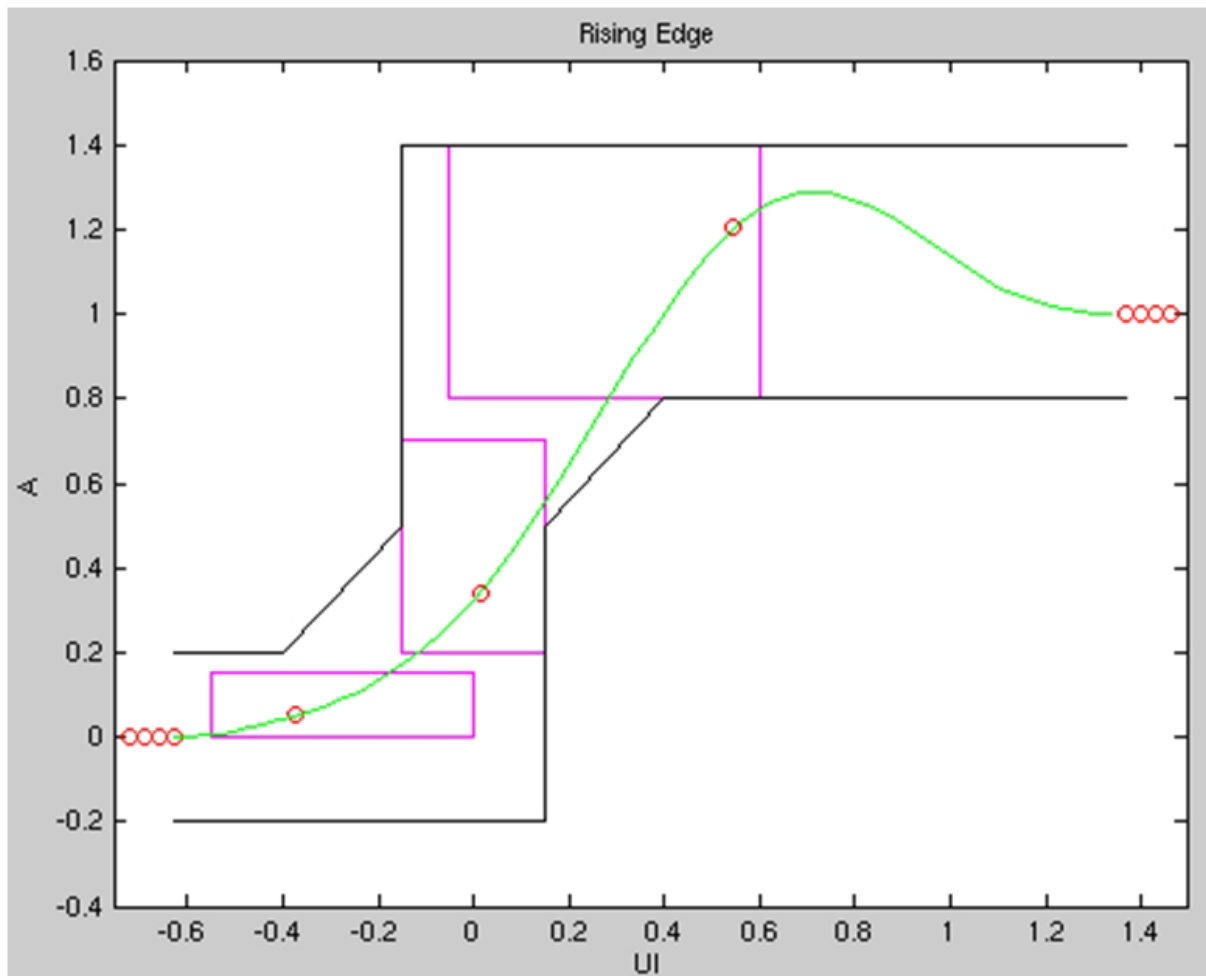


Figure 11-2: Polynomial interpolation for a rising edge pattern

11.2.2 Combining the Rising and Falling Edge with a pre-defined Bit-Pattern

For creating a SP2 pattern, pulse sequences of rising and falling edges are consecutively combined. The data structure is defined by a pattern file providing binary data sequences in Unit Intervals. The "MOST Stress Pattern" as well as user defined bit pattern can be used. The bit pattern must be offset free and the starting point must be equal to the end point to avoid Dirac impulses while using FFT. For every SP2 pattern one particular pulse shape of each, rising and falling edge, is used. Pulses of the pattern which are greater than 2 UI are connected by padding with either '1' or '0' between the rising or falling edges.

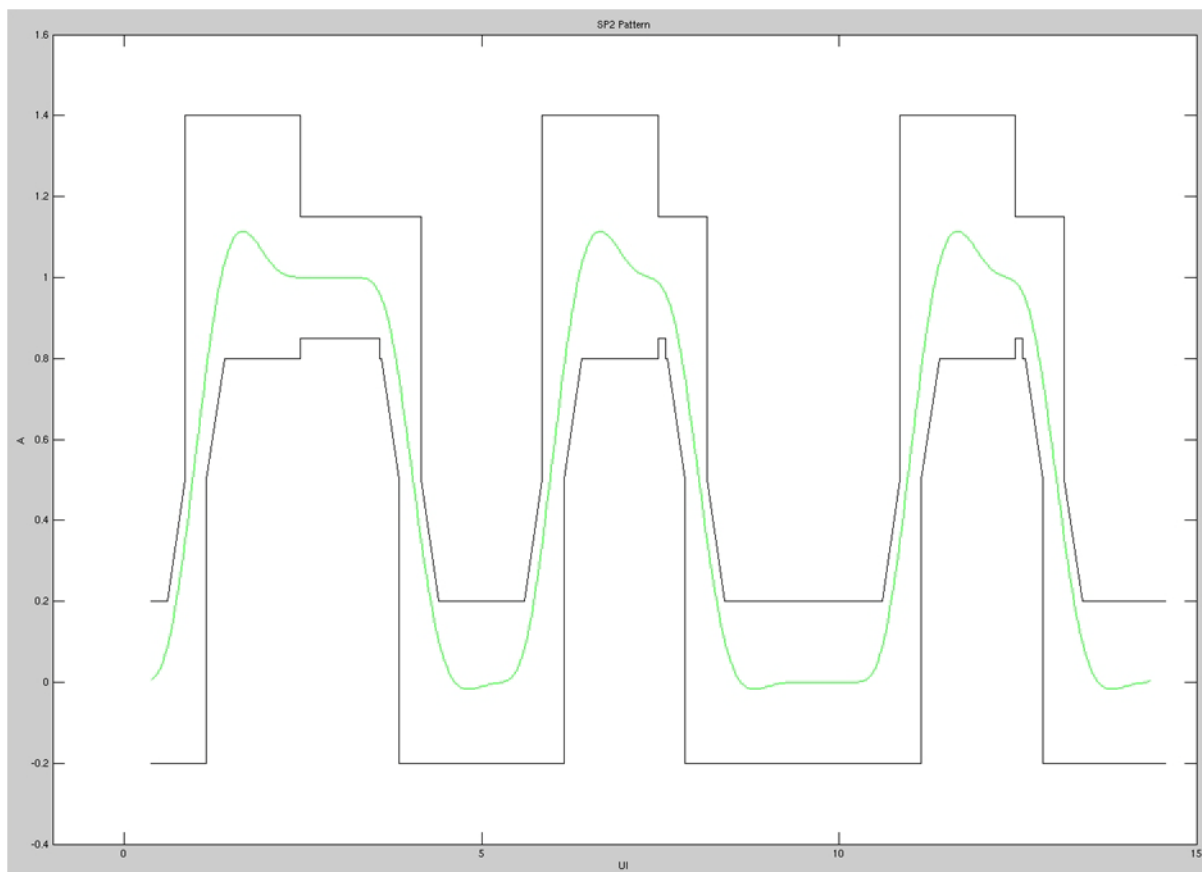


Figure 11-3: Generated SP2 pattern

Though all specifications for SP2 are fulfilled and the additionally defined constraints are matched, the resulting pattern might be idealistic compared to real optical transmitters used in the network. For instance, the bandwidth capabilities of optical transmitters is limited, the calculated patterns however might easily exceed this natural limitation. Besides all efforts to create worst-case patterns according SP2-Specification and to avoid unrealistic pulse shapes, the final database will contain scenarios that need to be excluded manually.

11.3 Calculation of the SP3 Pattern

A prediction for the scenario at the fiber output is calculated as the convolution of SP2 pattern and the POF's transfer characteristic defined in [3]. The generated SP3 pattern can be visualized and used for further analysis. A data-set, containing characteristic parameters for input and output parameters, is stored. This allows loading and also recalculation of the SP3 pattern together with any bit pattern.

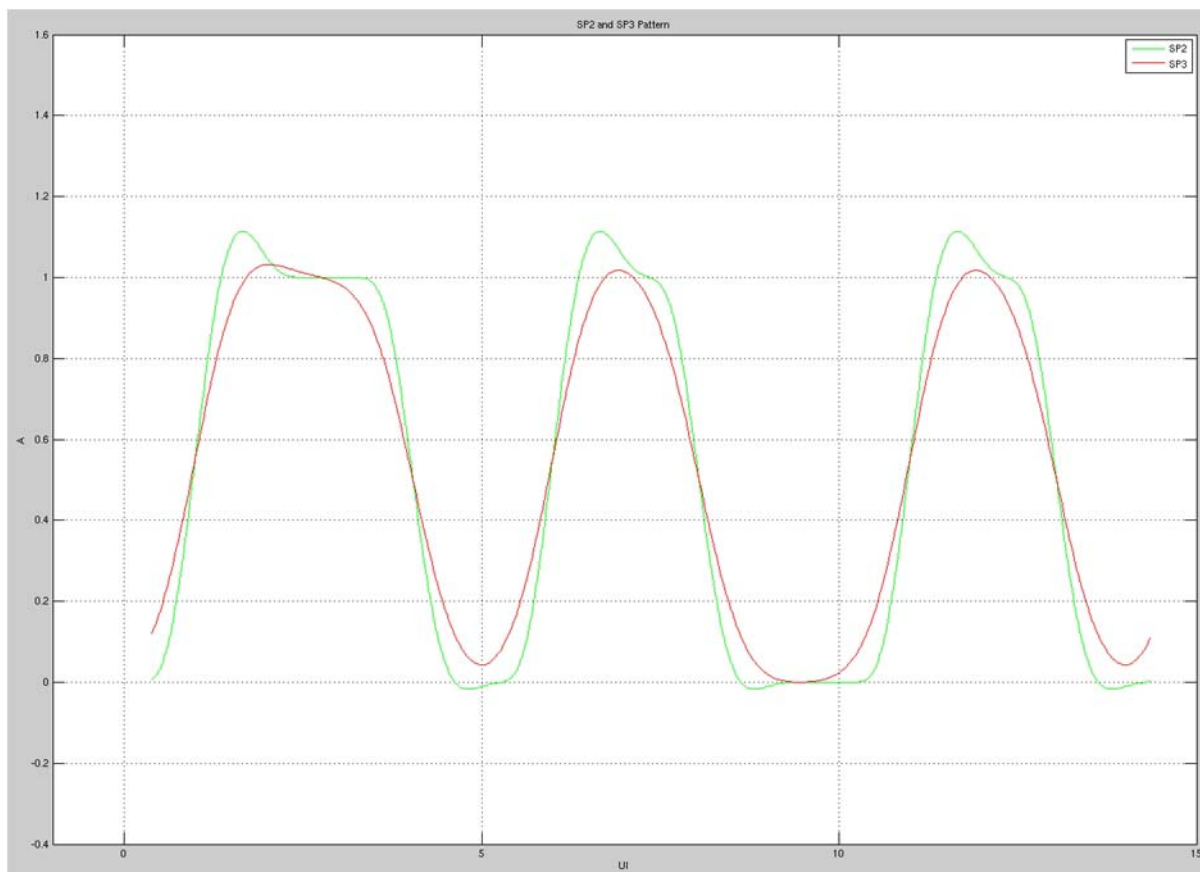


Figure 11-4: SP2 and SP3 pattern

11.4 Simulation and Analysis

The simulation program can generate multiple randomized rising and falling edges at once. Afterwards different SP2 patterns are generated using all permutations of the rising and falling edges together with a loaded pattern automatically. From this set of input pattern approximately 40,000 corresponding SP3 pattern can be calculated by a modern personal computer in one day. This leads to the calculation of millions of different SP3 pattern using multiple computers within a few days. The resulting pattern can be stored after simulation for further analysis and visualization.

Different parameters have been defined for SP3 pattern assessment (see below). These parameters are calculated for each SP3 pattern. Afterwards a defined number of worst-cases for each parameter are stored during simulation. If distributed calculation is used, the different simulations results can be merged.

- **Edge Min:** Minimum transition time of the SP3 pattern.
- **Edge Max:** Maximum transition time of the SP3 pattern.
- **Delta Edge:** Describes the maximum degradation in transition time.
- **Duty Cycle:** Maximum pulse width of a high or low pulse of the SP3 pattern.
- **Delta Duty:** Describes the maximum change in pulse width.
- **ISI Low:** amplitude deviation of SP3 pulses form steady state" B_0 "
- **ISI High:** amplitude deviation of SP3 pulses form steady state" B_1 "

As the determination of the worst-case pattern cannot be done analytically, all simulated patterns need to be investigated with respect to their coverage. Different plots (e.g. bar graphs) are provided to analyse and to visualize the coverage for the rising and falling edges as well as for the cross-coverage of the combined edges. In case of lacks in coverage, additional simulation runs with closed parameter bounds for better coverage can be performed.

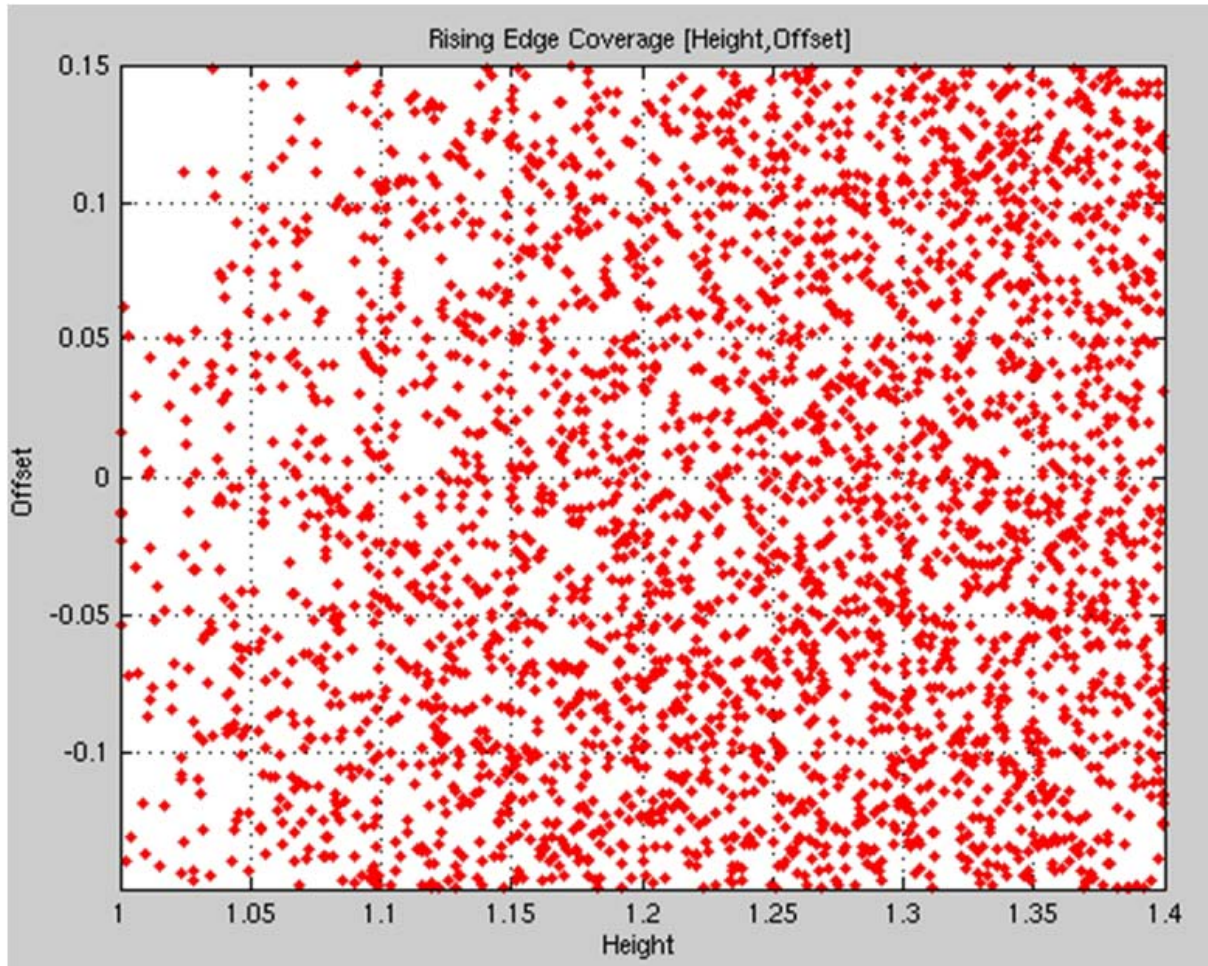


Figure 11-5: Rising edge cross-coverage for Height and Offset

11.5 Results

The simulation was performed for worst case POF conditions to find extreme input-conditions for the optical receiver. The chosen cut-off frequency represents the maximum specified fiber length of 15m and a numerical aperture of 0.5 for the launching condition at the fiber's input.

Due to the low-pass nature of the POF, degradation in transition times is visible. In extreme scenarios Inter-Symbol-Interference ISI was observed. Here, slow transition times are the root cause for reduced amplitude swing with short pulses, while longer pulses still achieve full amplitude swing. These effects may have negative impact on the conversion in the optical receiver following the POF. Signal/Noise ratio is directly degraded by ISI, additional Jitter may be generated in the optical-electrical conversion due to the slow transitions and ISI. A direct influence on signal timing due to the POF's bandwidth limitations was also detected. For instance, SP2 patterns with significant overshoots are supporting pulse spreading for positive pulses, which end up in a notable increase in Duty Cycle Distortion.

The extremes found based on a simulation run are listed in the following table:

Degradation in transition time

max

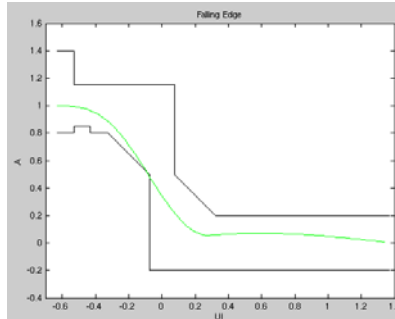
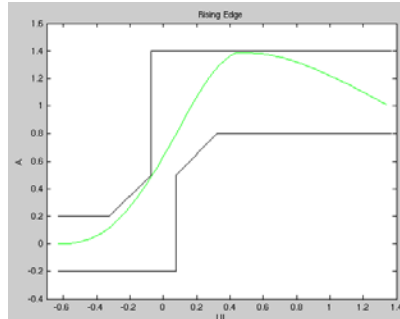
0.5UI

Example

Input rising edge (SP2)

Input falling edge(SP2)

Degradation on output (SP3)



*Rising edge degrades from
0.33UI → 0.62UI*

*Falling edge degrades from
0.34UI → 0.84UI
→ Delta 0.5UI*

Slowest transition time

max

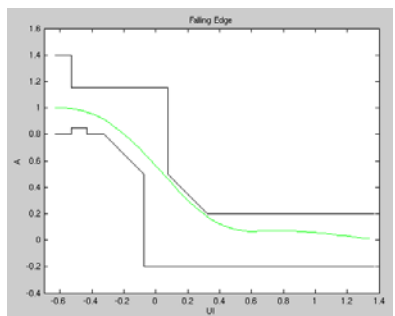
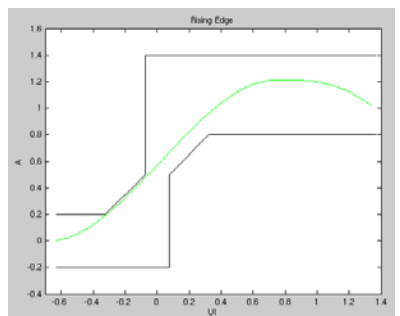
0.91UI

Example

Input rising edge (SP2)

Input falling edge(SP2)

Degradation on output (SP3)



*Rising edge degrades from
0.5UI → 0.75UI*

*Falling edge degrades from
0.5UI → 0.91UI
→ max 0.91UI*

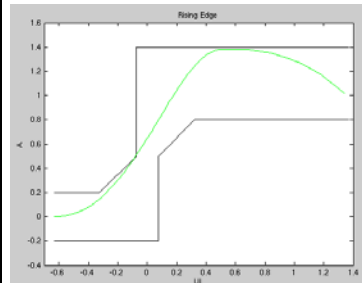
Duty Cycle Distortion DCD

max

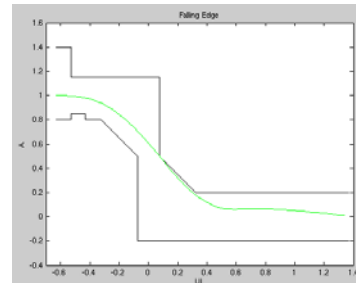
2.26UI

Example

Input rising edge (SP2)



Input falling edge (SP2)



Degradation on output (SP3)

For a 2UI-Pulse,
Pulse width spreads from
2.15UI → 2.26UI

→ max DCD of 2.26UI

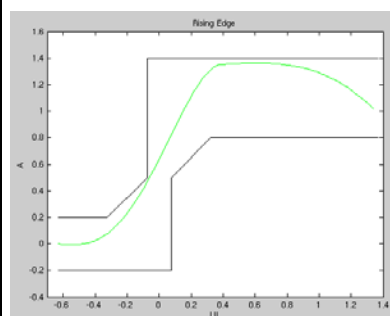
Delta Duty Cycle Distortion (Pulse Spreading)

max

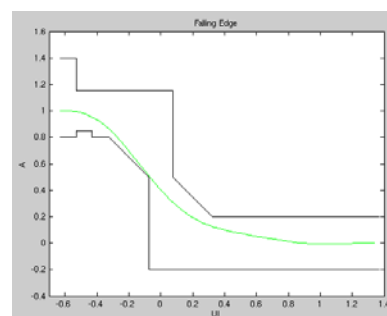
0.14UI

Example

Input rising edge (SP2)



Input falling edge (SP2)



Degradation on output (SP3)

For a 2UI-Pulse,
Pulse width spreads from
1.99UI → 2.13UI

→ max pulse spreading of
0.14UI

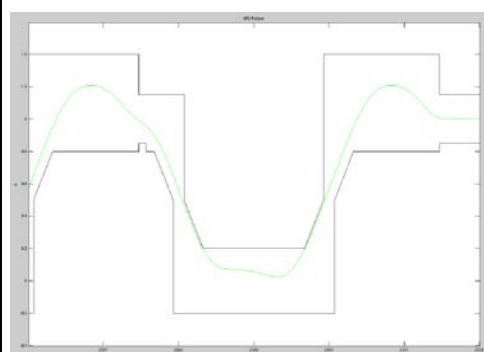
ISI, degradation of B_0 -level

max

0.096UI

Example

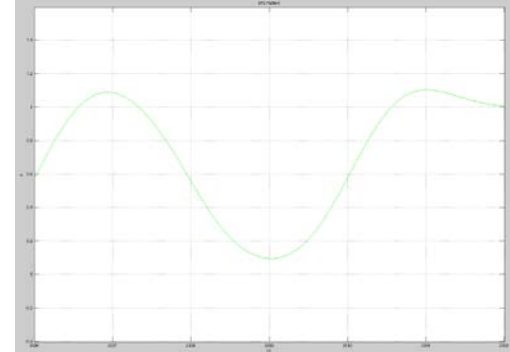
Pulse Shape, Input (SP2)



Degradation

B_0 -level is
shifted from
0.0UI
up to 0.096 UI

Pulse Shape, output (SP3)



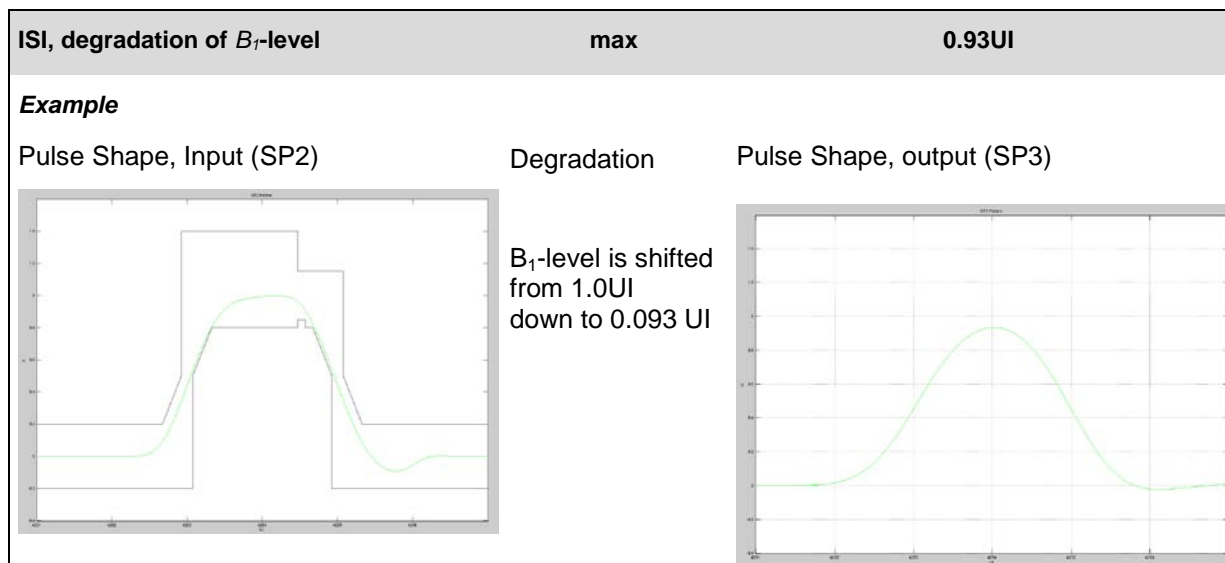


Table 11-1 Extreme pulse shape degradation due to bandwidth limitations

The detailed results of the simulation give clear indications on parameter variation and worst case scenarios. It also delivers SP3 test patterns which can be used for testing of optical receivers.

12 Appendix A: Index of Figures

Figure 5-1: Measured bandwidth versus POF-length (Luminous) for launching AN=0.5 with polynomial curve fitting	10
Figure 5-2: Comparing measured transfer function and Gaussian fit for 8m POF	11
Figure 5-3: Comparing measured transfer function and Gaussian fit for 10m POF	11
Figure 5-4: Comparing measured transfer function and Gaussian fit for 12m POF	12
Figure 5-5: Comparing measured transfer function and Gaussian fit for 14m POF	12
Figure 5-6: Comparing measured transfer function and Gaussian fit for 16m POF	13
Figure 5-7: Comparing measured transfer function and Gaussian fit for 20m POF	13
Figure 5-8: Comparing measured transfer function and Eq.(3.7) fit for 8m POF	14
Figure 5-9: Comparing measured transfer function and Eq.(3.7) fit for 10m POF	15
Figure 5-10: Comparing measured transfer function and Eq.(3.7) fit for 14m POF	15
Figure 5-11: Comparing measured transfer function and Eq.(3.7) fit for 16m POF	16
Figure 5-12: Comparing measured transfer function and Eq.(3.7) fit for 20m POF	16
Figure 6-1: Influence of numerical aperture on bandwidth parameters with polynomial approximations	18
Figure 6-2: Electrical 3dB-bandwidth versus launching aperture - measurement and approximation – various POF length.....	19
Figure 6-3: Three-dimensional view of 3dB-bandwidth B_{3dB} according to Eq.(6.5).....	20
Figure 10-1: Transfer function and simulated output signal; input signal without overshoot	22
Figure 10-2: Rise and fall time of input signal SIM slow (SP2)	23
Figure 10-3: Rise and fall time of output signal SIM slow_SP3	23
Figure 10-4: Eye diagram of input signal SIM slow (SP2).....	24
Figure 10-5: Eye diagram of output signal SIM slow_SP3	24
Figure 10-6: Transfer function and simulated output signal; input signal with overshoot	25
Figure 10-7: Rise and fall time of input signal SIM ov (SP2).....	25
Figure 10-8: Rise and fall time of output signal SIM ov_SP3.....	26
Figure 10-9: Eye diagram of input signal SIM ov (SP2)	26
Figure 10-10: Eye diagram of output signal SIM ov_SP3	27
Figure 10-11: Transfer function and simulated output signal; input signal with overshoot and deteriorated duty cycle	28
Figure 10-12: Rise and fall time of input signal SIM tst (SP2).....	28
Figure 10-13: Rise and fall time of output signal SIM tst_SP3.....	29
Figure 10-14: Eye diagram of input signal SIM tst (SP2)	29
Figure 10-15: Eye diagram of output signal SIM tst_SP3	30
Figure 11-1: Pattern parameter	35
Figure 11-2: Polynomial interpolation for a rising edge pattern.....	36
Figure 11-3: Generated SP2 pattern	37
Figure 11-4: SP2 and SP3 pattern	38
Figure 11-5: Rising edge cross-coverage for Height and Offset	39

13 Appendix B: Index of Tables

Table 1-1 Bibliography.....	5
Table 6.1: Values for measured and calculated bandwidths.....	19
Table 11-1 Extreme pulse shape degradation due to bandwidth limitations.....	42

Notes: